Universitat Autònoma de Barcelona

Master Thesis

The multifractal structure of ecosystems: implications for the response of forest fires to environmental conditions

Author:
Gerard M Rocher Ros

Supervisor:
Dr. Salvador Pueyo Puntí

A thesis submitted in fulfilment of the requirements
for the Master's degree in Modelling for Science and Engineering

in the

Department of Mathematics

developed at the

Institut Català de Ciències del Clima

July 2014

"Hom pot dir que la diversificació del medi i la interacció de les espècies entre elles i amb el medi, produeixen un cert ordre, lluny de la uniformització esperable en un model que considerés els individus de les diferents espècies com si fossin molècules d'un gas. La biosfera no és un sistema homogeni sinó que, cada punt, cada instant, té quelcom de particular: la flor, la molsa, un clot d'aigua, un raconet de bosc -o una ciutat-. La natura té una bomba d'entropia que l'aparta de la predicció d'uniformitat que pesa sobre sistemes senzills i tancats, almenys segons les interpretacions termodinàmiques corrents."

Ramon Margalef

"One can say that the diversification of the environment and the interaction of species among them and with the environment produce a certain order, far from the uniformity expected in a model that considers individuals of different species like gas molecules. The biosphere is not a homogeneous system but every spot, every moment has something special: the flower, the moss, a water puddle, a den of the forest, or a city. Nature has an entropy pump that chase away the prediction of uniformity weighing on simple and closed systems, at least according to the usual thermodynamic interpretations."

Ramon Margalef

UNIVERSITAT AUTÒNOMA DE BARCELONA

Abstract

Sciences Faculty
Department of Mathematics

Master's degree in Modelling for Science and Engineering

The multifractal structure of ecosystems: implications for the response of forest fires to environmental conditions

by Gerard M Rocher Ros

Ecosystems are generally arranged in complex patterns, and often this is due to self-organisation processes. The main characteristic of a self-organised system is that interactions of the smaller components of the system produce emergent properties that are only seen at a larger scale. Also, many self-organised systems present scale invariance, that is, any part at any scale resembles the whole. This is characteristic of a fractal object.

In this thesis, I study the landscape of ecosystems under a fire regime using multifractal analysis. I show that those ecosystems are self-organised, displaying multifractal patterns in the landscape, both when simulated with a model and in real data of boreal forests.

Furthermore, I explore, for the first time, the relationship of multifractal patterns with the external forcing that drives the system, showing that the multifractal structure that constitutes the ecosystem makes it sensitive to the environment.

This has implications for the study of self-organising processes and also for ecological studies, as it relates the structure of the system to the mechanisms that drive it.

Acknowledgements

I am very thankful to the colleagues of the master, specially Oriol, Genís, Aina and Yann, with who I shared an interesting year into a new world for me. Also to David, Helena, Ruben, Lluïsa, Àlex i Gigi, who support me despite they were not sure what I was doing this year.

I would like to thank also my family, *papes*, Berta, Vidalba and the newborn Dàlia, who encouraged me to go forward in this direction. Specially to Inga, who has always been there.

I want to acknowledge Kathy Schon from the USGS for her help with the data. I am also thankful to Antonio Turiel for his comments. And to the people of IC3 with who I shared the last months.

I also want to mention Ramon Margalef, whose books and ideas led me from the environmental sciences to the magical world of complex systems. This trip would haver never been possible without Salvador Pueyo, who showed me the path to this world, and helped me to see the reality from another point of view, with infinite dimensions and through all scales. Thank you for being a great advisor and a better friend.

Contents

Abstract ii

Acknowledgements iii

Contents iv

List of Figures vi

Abbreviations vii

Symbols viii

1 Introduction and background 1
- 1.1 Self-organisation, criticality and scale invariance . . . 1
  - 1.1.1 Self-organisation and criticality . . . 1
  - 1.1.2 Scale invariance, fractals and power laws . . . 2
- 1.2 Forest fire models . . . 4
  - 1.2.1 Henley, Drossell and Schwabl's model . . . 4
  - 1.2.2 The SOCFUS model . . . 6
  - 1.2.3 Results of Pueyo's [2007] work . . . 7
- 1.3 Multifractals . . . 9
  - 1.3.1 Multifractals in space, the example of mineral distribution . . . 10

2 Methods 12
- 2.1 Multifractal spectrum . . . 12
  - 2.1.1 The method of moments . . . 14
  - 2.1.2 The cumulative probabilities method . . . 15
- 2.2 Temporal evolution of the model . . . 16
- 2.3 The empirical data . . . 17
  - 2.3.1 From fuel types to rates of spread . . . 18
  - 2.3.2 Acquisition and processing of the data . . . 19
- 2.4 The critical value of the SOCFUS model . . . 21

3 Results 22
- 3.1 Multifractal structure of the forest . . . 22
  - 3.1.1 Multifractal structure of the landscape emerged from the SOCFUS model . . . 22

3.1.2 Multifractal structure of fuel types in boreal forests in Alaska . . . 28
3.2 Temporal evolution of the SOCFUS model . . . 30
3.3 From the multifractal spectrum to the power law exponents . . . 34
3.3.1 The critical value of the SOCFUS model . . . 34
3.3.2 Exponents of the power laws and the decomposition of the multifractal spectrum . . . 35

4 Discussion **38**
4.1 Multifractal patterns in ecosystems . . . 38
4.1.1 Multifractality of the landscape of self-organised ecosystems . . . 38
4.1.2 Multifractality of a SOC system over time . . . 40
4.2 Environmental conditions decompose the multifractal spectrum . . . 41
4.2.1 Implications for climate change: the megafire . . . 42
4.2.2 Insights for forest management . . . 43

5 Conclusions **45**

Bibliography **47**

List of Figures

1.1 The nature is fractal: A fjord from Norway . . . 3
1.2 Main results of Pueyo [2007] . . . 8
1.3 Landscape emerged from SOCFUS model . . . 10

2.1 Historical fires in the selected area of Alaska . . . 20

3.1 Plot of $\chi_q(\varepsilon)$ vs ε from the model . . . 23
3.2 Plot of the Hölder exponents, α versus q . . . 24
3.3 Histogram of μ . . . 25
3.4 The multifractal spectrum from the model . . . 26
3.5 Comparison of both methods to calculate the multifractal spectrum . . . 27
3.6 Map of fuel types of the area of study . . . 28
3.7 Plot of $\chi_q(\varepsilon)$ vs ε from the empirical data . . . 29
3.8 The multifractal spectrum from the landscape on Alaska . . . 30
3.9 Temporal evolution of the model . . . 31
3.10 Relationship between $\tau''(1)$ and S. . . . 32
3.11 The emergence of multifractality . . . 33
3.12 Histogram of r_i . . . 34
3.13 Relationship between r_e and β. . . . 35
3.14 Relationship between β and $f(\alpha)$. . . . 36
3.15 Relationship between r_e and $f(\alpha)$. . . . 37

4.1 Comparison of multifractal spectrums. . . . 39

Abbreviations

FF	Henley, Drossell and Schwabl's '**F**orest **F**ire' model
FWI	Canadian **F**ire **W**eather **I**ndex
LANDFIRE	**Land**scape **Fire** and Resource Management Planing Tools
RFM	**R**othermel Mathematical **F**ire **M**odel
SOC	**S**elf-**O**rganised **C**riticality
SOCFUS	**S**elf-**O**rganised **C**ritical **Fu**el **S**uccession model
USGS	**U**nited **S**tates **G**eological **S**urvey

Symbols

BA	Burnt area since the previous fire
D	Fractal dimension
D_E	Euclidean dimension
I_R	Reaction intensity of the RFM
L	Size of the bidimensional lattice
$N_\alpha(\varepsilon)$	Cumulative number of boxes of size ε with certain α
Q_{ig}	Heat of preignition for the RFM
S	Shannon entropy
T_{r_i}	Sum of all r_i in a matrix
a	Constant of the power law
$f(\alpha)$	Singularity spectrum
g	Fuel accumulation between two ignitions
$n_\alpha(\varepsilon)$	Number of boxes of size ε with the same α
$p(\alpha)$	Probability to find a given α
q	Order of the moment of $\chi_q(\varepsilon)$
r	Probability of fire propagation in a cell of SOCFUS model
r_c	Critical r
r_e	External or *environmental* component of r
r^e_{min}	Maximum r_e
r^e_{max}	Minimum r_e
r_i	Internal or *fuel* component of r
r_∞	Limit of r_i
r_s	Fire spread rate of the RFM

$\propto$	Indicates proportionality
α	Hölder exponent or singularity strength
β	Slope parameter of the power law distribution of fire sizes
γ	Probability of a tree 'appearing' in an empty cell in FF model
ϵ	Effective heating number for the RFM
ε	Size of the box
η	Rate of ignition of FF model
θ	Probability distribution function
κ	Parameter of r_e
$\mu_{i,j}$	Normalized measure of $r^i_{i,j}$
$\mu_{m,n}(\varepsilon)$	Sum of the measure of $\mu_{i,j}$ in a box of size ε
ξ	Propagating flux ratio
ρ_b	Fuel bulk density of the RFM
$\tau(q)$	Exponent of the power law obtained from $\chi_q(\varepsilon)$
$\tau''(1)$	Multifractal measure according to Cheng [1994]
ϕ_s	Slope coefficient of the RFM
ϕ_w	Wind coefficient of the RFM
$\chi_q(\varepsilon)$	Mass-partition function of μ
$\Psi(\alpha)$	(Corrected) probability distribution function of α

Chapter 1

Introduction and background

In this thesis, I explore the multifractal structure that lies beneath the ecosystems, from the point of view of forests fires. I use a simple model that simulates forest fires and ecological succession, and also empirical data from an area that is known to suffer frequent fires.

In the following section I introduce the reader to the main concepts of self-organisation, fractals and multifractals, and some necessary background of forest fire models, specially the work developed by Pueyo [2007] which is the basis of this thesis.

1.1 Self-organisation, criticality and scale invariance

1.1.1 Self-organisation and criticality

Most of the systems that compose our universe are formed by a large number of entities, with complex interactions and very often nonlinear dynamics. The classical approach to study any system is to understand the composition, state and the evolution of the system, or the parts that compose it. But due to the large number of particles and interactions, those systems cannot be studied with classical physics, as it is almost impossible to know the states of each particle and predict its particular evolution in order to calculate the interactions and obtain the general state of the system. The discipline of statistical physics deals with this problem, using the large amount of particles of the

system not as a problem but as a useful fact, because, in this situation, statistical tools give accurate predictions and analyses of the system.

Furthermore, many of these systems, as it is clear in ecology, show many interactions among different elements of the system, with emergent properties that are not possible to identify at the individual level. Some dissipative systems, far from thermodynamical equilibrium and with many degrees of freedom, show a variety of complex patterns, reaching a state of self-organisation, and they self-regulate to remain in that state.

Bak et al. [1988] developed a new concept, *Self-Organised Criticality* (SOC) to describe some of those systems, as there is a critical point where the system naturally self organises.

Precisely, the definition of self-organisation is that the interaction of the smaller components of the systems produces emergent properties that are only appreciable at the larger scale.

SOC have been claimed in a large number of fields, such as astrophysics, geophysics, particle physics, ecology, biology, social systems... [Aschwanden, 2013], and in all these kinds of systems it is possible to find similar patterns and behaviours. Therefore it is a good starting point to find general rules in nature, although there is self-organisation without criticality [Pueyo et al., 2010], and many other theories from complex systems that can provide useful explanations to those processes.

1.1.2 Scale invariance, fractals and power laws

SOC systems have other interesting properties. When self-organised, they display scale invariance. That is, the pattern found at a certain scale is similar as we zoom in or either out; i. e. the system is scale free: there is not any characteristic scale to represent the system.

This kind of structure was studied in detail by Mandelbrot [1982], naming it *fractal*. Those patterns are striking structures, where any part resembles the whole. Fractal shapes are found throughout the natural world, i. e. the coast of an island [Mandelbrot, 1967], river networks [Tarboton et al., 1988], trees, the blood vessel system, the lungs, or the universe itself [Iovane et al., 2004].

Mandelbrot [1982] developed a set of mathematical tools to deal with those objects. The main concept that emerges from his work is that those objects have a fractal dimension

D, which can be a non-integer number, and is a measure of how the object fills the space. For example, a tree with few branches, although self-similar and fractal, has a lower D than another with a large number of branches that fill very well the space. Or the coast of Brazil, smooth and with long beaches, has a lower D than the Norwegian coast with endless fjords (figure 1.1). Note that D is always $\leq D_E$, where D_E is the Euclidean dimension of the object.

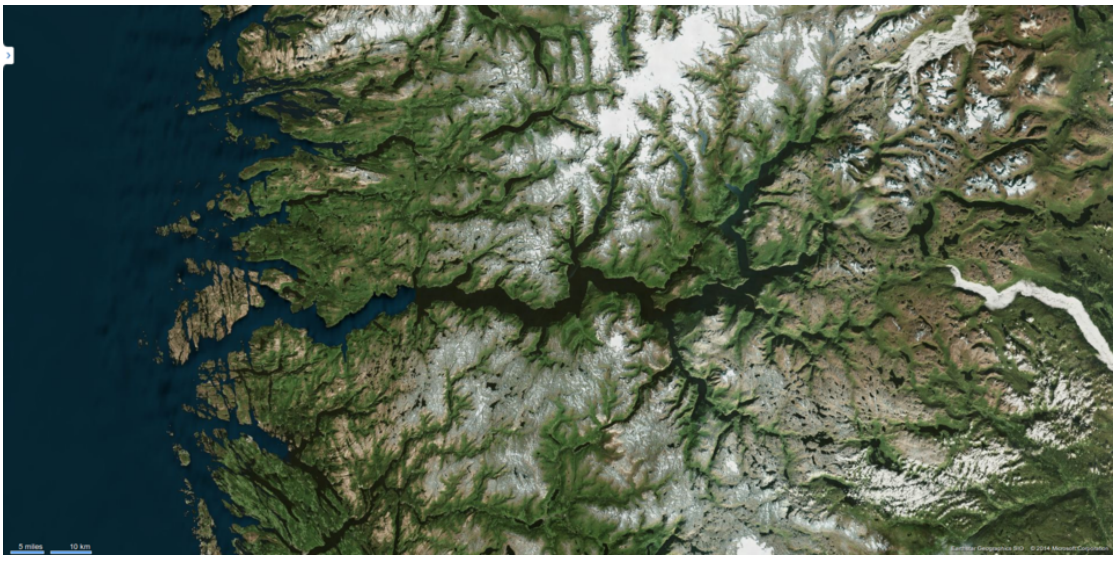

FIGURE 1.1: The nature is fractal: a satellite image of the largest Fjord in Norway, the Sagnefjord. Several fractal objects are visible: the fjords, the mountain ranges, the river networks; the distribution of islands, lakes, or glaciers.

The statistical distribution that is inherent to fractal and scale free objects is the *power law*:

$$\theta(s) \propto as^{-\beta} \tag{1.1}$$

Where a is a constant, s is the size of the measure and $\theta(s)$ the frequency of this measure. This distribution is characterized by a large amount of smaller size elements, and just a few of very large ones. Thinking about a river network, there is just one river with the largest width, but hundreds of streams with less than 100 cm.

The scale invariance of the power law is better seen when the measures are represented by logarithms, as changing the scale is precisely increasing the logarithm of a measure. Therefore, a power law representing certain measure of a fractal object in a log-log plot appears as a straight line, and precisely the slope of this straight line, $-\beta$, where β is the exponent of the power law which is related to the fractal dimension D.

1.2 Forest fire models

In order to study self-organisation processes, Bak, Tang, and Wiesenfeld first introduced the sandpile model, which naturally evolves to a critical state, without fine tuning of the parameters of the model. This was the first model to reproduce SOC, but other models for earthquakes [Olami et al., 1992], evolution of populations [Bak and Sneppen, 1993] or cloud formation [Nagel and Raschke, 1992] also reproduce this behaviour.
Another example is the forest fire model in Drossel and Schwabl [1992], Henley [1993]. In the next section the main characteristics and behaviour of this model will be explained. There are, though, three characteristics of forest fire dynamics that indicate it can be a self-organised critical system:

1. Is a multiplicative phenomenon (fire spreads).
2. Can have negative feedbacks (burnt areas preventing future fires in the long term).
3. Time scales are separated.

It can be true for large, undisturbed forests of certain areas, like boreal or temperate forests. Although in other biomes it may not be the case, for example, the Amazonian rain forests [Pueyo et al., 2010].

1.2.1 Henley, Drossell and Schwabl's model

Drossel and Schwabl [1992] and Henley [1993] developed the *"Forest Fire"* (FF) model which simulate self- organisation processes in a forest under the influence of forest fire. It is a very simple model, inspired in the idea of forest fires, but does not pretend to reproduce the behaviour of fires as it is too simple for that, and comprises some unrealistic properties that do not allow it to be used to model real fire dynamics. However, it has very interesting properties related to self-organisation.

The model can be summarized as follows:
In a bidimensional lattice, each cell can be in one of three states: empty, with a tree, or with a burning tree. In a time step, an empty cell can get a tree with a probability $\gamma \ll 1$, and if there is a tree on the cell, can be hit by lightning and become a burning tree with probability $\eta \ll \gamma$. Then, if there is a burning tree in a cell *(i,j)* at a time step,

the fire spreads to each of the neighbouring cells if that have a non burning tree. In the model, fire can spread to the four nearest neighbours *(i-1,j), (i+1,j), (i,j-1), (i,j+1)*. Also, at this time step where fire spreads to a neighbour cell, the cell *(i,j)* becomes empty. The fire will stop when there are no neighbours with a tree where it can spread. As long as there is a fire burning, there are neither lightning strikes nor tree growth in the lattice. This property is important as it allows the model to separate the different phenomena that happen at different time scales, that is, fire spreads at a time scale in which tree growth is negligible.
This model captures two important properties of ecological processes:

- Ecological *constructive processes* are rather slow, while catastrophic events are fast [Margalef, 1997].
- The two dimensions allow the arrangement of groups of trees, introducing spatial correlations.

But on the other hand, there are several features that make the model too unrealistic to really represent the ecological processes of forest fires.

- Trees do not appear randomly and with a unique size. There is a fuel succession where biomass increases gradually.
- The fire spread does not depend only on the presence of a tree in a cell, but on the properties of the vegetation, specially the type and amount of fuel, among others. And specially it also depends on environmental conditions such as wind, moisture and temperature.

In order to better recreate the fire dynamics and its statistical properties, Pueyo [2007] developed a variant of the FF model, the ***S****elf-****O****rganised* ***C****ritical* ***Fu****el* ***S****uccession model* (SOCFUS).

1.2.2 The SOCFUS model

The SOCFUS model, developed by S. Pueyo, and fully studied and detailed in Pueyo [2007], maintains the original simplicity of the FF model dynamics, but it captures some essential properties of real forest fire ecological processes.

The most important improvement is that each cell of the lattice is no longer binary (presence/absence of trees), but now the ecological succession is represented. A probability r of catching a fire is assigned at each cell, either from the ignition (lightning) or from neighbouring cells when fire spreads. The value of r increases gradually over time and decreases abruptly when the cell is burnt; this component captures the essential part of fuel succession, as there is evidence that in boreal forests, fire risks increases over time [Niklasson and Granström, 2000]. Interestingly, Pueyo [2007] states that there were no clear differences between the behaviour of FF and SOCFUS model, indicating that, as statistical physics suggests, SOC systems are universal and in this case both models belong to the same "universality class". But additionally, the SOCFUS model can be used to study fuel succession in forest fire dynamics.

Another new rule added to the model is that the probability r of catching a fire is composed of two parts:

$$r = r_i + r_e \tag{1.2}$$

- r_i represents the *internal* component of the probability of burning of each cell (i. e. the "amount" of fuel), increases gradually over time and if it is burnt becomes 0.
- r_e represents the *external* component of the probability of burning, and is independent of the cell. It simulates the *environmental* component of forest fires, as real world fires depend not only on the fuel but also on the meteorological conditions.

Equation 1.2 is constrained by $r \in [0, 1]$, and $r_i \in [0, r_\infty]$, where r_∞ is a predefined threshold (in this case, $r_\infty = 0.7$).

r_e follows a truncated exponential distribution, $\theta(r_e) \propto e^{\kappa r_e}$, with $r_e \in [r^e_{min}, r^e_{max}]$.

Is important to note that r_i depends on each cell *(i,j)*, but for a certain fire, r_e will be fixed: the same "environment" for all cells while the fire spreads.

The sequence of the fire spread is the same as in the FF model, but now the spread of a burning cell to a neighbour cell *(i,j)* depends on a probability $r^{ij} = r^{ij}_e + r^{ij}_i$ instead of

presence/absence of a tree. The sequence will end when there is not any cell with fire. Then, all cells burned will have $r_i^{ij} = 0$, and all r_i^{ij} are increased by a certain amount g (proportional to the time between each lightning, as we assume that r_i increases at a constant rate).
For more information about the implementation of the model and the details of the algorithm, see Pueyo [2007].

1.2.3 Results of Pueyo's [2007] work

The results obtained by Pueyo [2007], using the SOCFUS model and empirical data from boreal forests in Alberta, Canada, are the motivation of this project. Here the main findings will be explained in order to stablish the framework of this master thesis. As explained in section 1.2.2 above, the SOCFUS model allows us to study fire dynamics with fuel succession mechanisms included, which could play a central role in real world fires. Also, the other important component is included: the environmental forcing. This is not only useful to recreate more accurately the reality in the model, but also allows to compare the modelled results with empirical data, and therefore understand the mechanisms in real forest fires. We should not forget that a model is a simplification of reality to be able to understand the real world.

As forest fires, at least in some areas, seem to display SOC behaviour (or more accurately, *Self Organised sub-Criticality*, as the system self organises below the critical point [Pueyo, 2007]), their sizes are well described by a power law distribution, eq. 1.1, and specially by the slope of the power law represented in a log-log plot, β.
With the SOCFUS model, Pueyo [2007] found that different environmental conditions r_e, are related with different fire size distributions, expressed as different power laws (**a** of fig. 1.2). Furthermore, he compared the results with an empirical proxy to r_e, the Fire Weather Index (FWI), which summarizes meteorological variables that are related with fire risk, specially fuel moisture. Using the FWI together with empirical values of β, he compared the results of the SOCFUS model with reality, showing a clear relationship between both (**b** and **e** of fig. 1.2).
An interesting finding is that, as r_e increases, that is, environmental conditions are more favourable for fire, the slope β of the fire distribution decreases, meaning that large fires are more probable (**b** and **c** of fig. 1.2).

A similar relationship is established with empirical data (**d**, **e** and **f** of fig. 1.2).

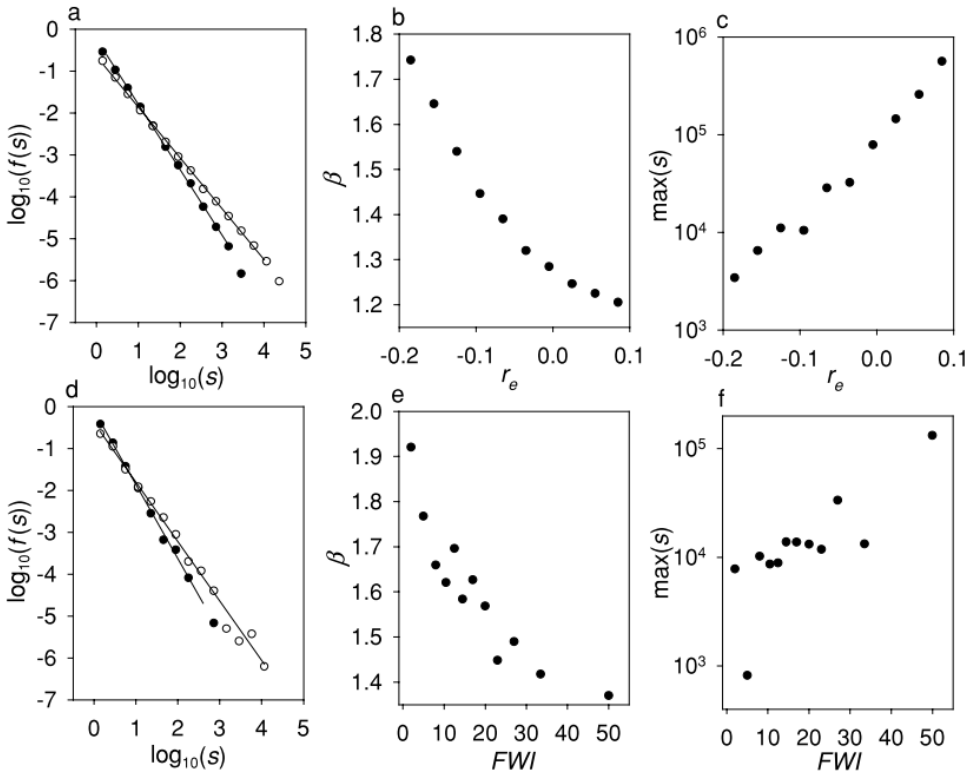

Fig. 5 The short-term effect of environmental fluctuations on fire regime in a simulation and a real case. The simulation is experiment 1, Section 3.3. The empirical fires are the 3,134 fires that burned at least 1 ha in Alberta's Forest Protection Area from 1983 to 1995. The environmental term for the empirical fires is the Canadian Fire Weather Index (*FWI*) (Section 4). (a) The probability density function of simulated fire sizes, with environmental parameter r_e from -0.14 to -0.11 (*solid circles*) and r_e from 0.01 to 0.04 (*open circles*). (b) The relationship between r_e and the slope parameter β in simulated fires. (c) The relationship between r_e and the size of the largest simulated fire max(s). (d) The probability density function of empirical fire sizes in hectares, with *FWI* from 4 to 6 (*solid circles*) and *FWI* from 30 to 37 (*open circles*). (e) The relationship between *FWI* and β in empirical fires. (f) The relationship between *FWI* and the size of the largest observed fire max(s) (hectares) in empirical fires

FIGURE 1.2: Reproduction of figure 5 of Pueyo [2007], summarizing the main findings of his work.

Salvador Pueyo stated two hypotheses that will be tested in this master thesis:

- The forest is self-organised, arranged in a multifractal structure.
- Environmental conditions, r_e, decompose the multifractal spectrum of the forest in different scaling sets.

1.3 Multifractals

In section 1.1.2 I briefly introduced the concept of fractals to describe the shapes that surround us. Fractal structures are anywhere in the universe, and have been proven to be very useful to describe systems. However, sometimes a scale-invariant object cannot be defined by only one fractal dimension D, as it may be shaped by multiple, or infinite fractal dimensions.

In his main book, Mandelbrot [1982] states that a single D may not be sufficient, but the concept of multifractal was later developed and popularized in the research area of turbulent behaviours. Already on 1941, Kolmogorov [1941] had the intuitive idea that under fully developed turbulence, a case of a physical scale invariant system, energy was transmitted from large scales to small ones by a variable that only depends on the quotient of both scales. The physical variables then are associated to a fractal or multifractal structure beneath [Turiel et al., 2006].

Multifractal patterns can be found also in a wide variety of objects, ranging from time series of rainfall [Dauphiné, 2013], heartbeat dynamics [Ivanov et al., 1999], or different spatial patterns such as forest gaps in the rain forest [Solé and Manrubia, 1995] or in mineral deposits distribution [Agterberg, 1995]. This latter case is a good example related with this work, and will be explained in more detail in the next section.

1.3.1 Multifractals in space, the example of mineral distribution

Mandelbrot [1989] states the importance of the multifractal formalism in geophysics, as many geochemical or geological properties are multifractally distributed, he suggests. A simple example to realize this is the case of copper [Mandelbrot, 1989], quoting his own words:

> *"High-grade copper is of course distributed nonuniformly: it concentrates in few regions of the world. If one examines such region in detail, however, copper continues to be found nonuniform: it concentrates in few sub-regions. And so on. It is reasonable, therefore, to suppose that the relative distribution of high-grade copper is the same (in the statistical sense) within each copper-bearing region, whether is small or large.[...] Next, examine lower grade copper. The fact that is more widespread in nature is expressed by its being supported by a fractal set of higher fractal dimension. Overall, in order to give a full representation of copper it is seen that fractals are necessary and no single fractal set is sufficient."*

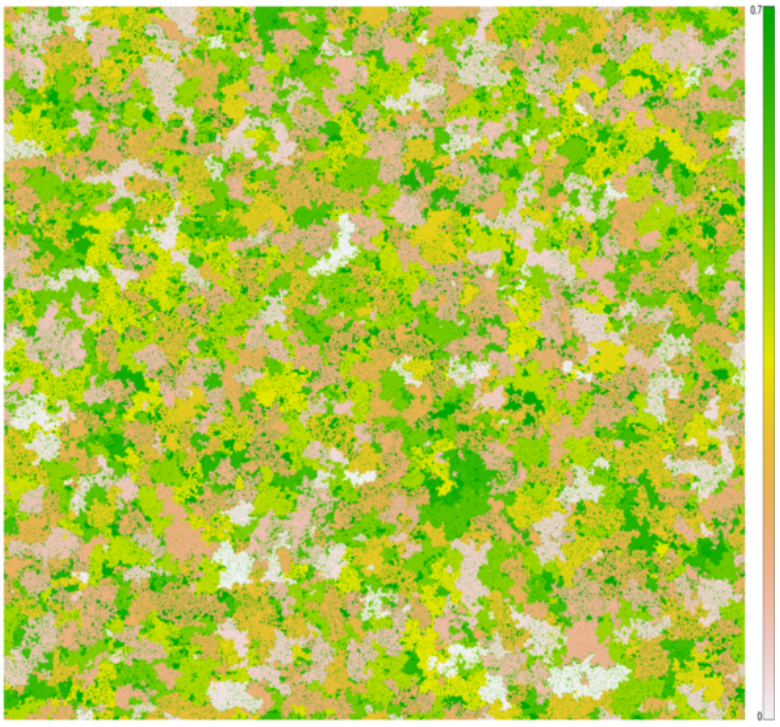

FIGURE 1.3: Image of the landscape emerged from SOCFUS model, showing different values of r_i, the amount of fuel in each cell. Lattice size of 2048x2048.

It is clear then that some objects require more than a fractal set, and the group of those fractal dimensions is defined as a *multifractal measure.* The mathematical and statistical aspects of multifractals will be explained in section 2.1.

The SOCFUS model originates a complex landscape, a "patchy-like" structure (fig 1.3), where different amounts of *fuel* (not exactly fuel, but probability of catching fire dependent on the fuel), r_i, are represented. This structure is expected to be multifractal. This is easy to understand if we think of the fuel distribution on the landscape as the example of copper distribution from Mandelbrot [1989]. Considering a certain measure of r_i, will be distributed according to a particular fractal dimension, and maybe another measure of r_i will be more common on the landscape, e. g. a higher fractal dimension. Considering that r_i is continuous in $\in [0, r_\infty]$, to describe the spatial distribution of r_i an infinite number of fractal dimensions could be required. Hence, it might be multifractal.

Chapter 2

Methods

2.1 Multifractal spectrum

In order to study the hierarchical structure of the landscape, consider a square matrix of size L, where each cell has a $r_i^{i,j}$ assigned (a certain amount of the *internal* component of the probability of burning for a *(i,j)* cell). In those simulations, $L = 2048$.
Now, to normalize the matrix we define a new measure,

$$\mu_{i,j} = \frac{r_i^{i,j}}{T_{r_i}} \tag{2.1}$$

Where $T_{r_i} = \sum_{i=0}^{L}\sum_{j=0}^{L} r_i^{i,j}$ is the sum of all values, in order that $\sum_{i=0}^{L}\sum_{j=0}^{L} \mu_{i,j} = 1$.
Let us cover the map with boxes of size ε, with varying sizes of ε in order to have different scales. For simplicity, ε can take values as 2^n, where $0 \leq n \leq 11$, so ε can be 1, 2, 4, 8, 16...512, 1024, 2048.
Let the measure $\mu_{m,n}(\varepsilon)$ be the total measure of $\mu_{i,j}$ in a box of size ε,

$$\mu_{m,n}(\varepsilon) = \sum_{i=0}^{\varepsilon}\sum_{j=0}^{\varepsilon} \mu_{i,j}$$

As $\mu_{i,j}$ will be distributed non-uniformly on the space at all scales, $\mu_{m,n}(\varepsilon)$ will follow a power law with ε in the limit of box size $\varepsilon \to 0$,

$$\mu_{m,n}(\varepsilon) \propto \varepsilon^{\alpha_{m,n}} \tag{2.2}$$

where $\alpha_{m,n}$ is called the Hölder exponent [Mandelbrot, 1989], or *strength of singularity* [Frisch and Parisi, 1985].

Then, different boxes $\mu_{m,n}$ of size ε have different values of the Hölder exponent $\alpha_{m,n}$. Let us define the number of boxes with a specific α value as $n_\alpha(\varepsilon)$. If $n_\alpha(\varepsilon)$ follows a power law with scale ε,

$$n_\alpha(\varepsilon) \propto \varepsilon^{-f(\alpha)} \tag{2.3}$$

It is clear that the boxes with the same Hölder exponent α form a particular fractal set. The exponent $f(\alpha)$ can be thought as the Hausdorff fractal dimension of α, but this is not entirely accurate, as it is possible to have negative values, while negative fractal dimensions are not realistic [Mandelbrot, 1989].

$f(\alpha)$ may not only be seen as a mathematical function but from a probabilistic point of view, as

$$f(\alpha) = D_E + \Psi(\alpha) \tag{2.4}$$

[Mandelbrot, 1989], where D_E is the Euclidean dimension of the object and

$$\Psi(\alpha) = \frac{\log(p(\alpha))}{\log(L/\varepsilon)} \tag{2.5}$$

which is simply an expression of the probability of α.

More details about $f(\alpha)$ can be found in Mandelbrot [1989] and also Halsey et al. [1986], and will be better explained in section 2.1.2, but in most of the cases, and for a better interpretation, $f(\alpha)$ can be treated as the fractal dimension of a measure α, and the relationship of α and $f(\alpha)$ is defined as the multifractal spectrum.

Different methods to estimate the multifractal spectrum have been developed. The method of moments was introduced by Halsey et al. [1986], and other methods in order to deal with natural images have also been developed. More information of different methods are detailed in Turiel et al. [2006]. While other methods provide more accurate estimates of the multifractal spectrum, the method of moments is particularly helpful to investigate if the system is scale invariant, and in which range of scales shows multifractality.

2.1.1 The method of moments

To be able to calculate the multifractal spectrum I used the method of moments.
A mass-partition function of the moment of order q is defined as

$$\chi_q(\varepsilon) = \sum_{N(\varepsilon)} \mu_{m,n}^q(\varepsilon) \tag{2.6}$$

The sum is done for all boxes of size ε, with $-\infty < q < +\infty$. It is interesting to note that for $q = 0$, we are simply calculating the fractal dimension, D.
For $q = 1$ is the Shannon entropy:

$$S = -\sum_{N(\varepsilon)} \mu_{m,n} \log(\mu_{m,n}) \tag{2.7}$$

And for $q = 2$ is in fact related to the variance and to the correlation dimension [Solé and Manrubia, 1995]:

$$C_d = \frac{\log\left[\sum_{N(\varepsilon)} \mu_{m,n}^2\right]}{\log(\varepsilon)} \tag{2.8}$$

Then, for large, positive values of q the sum is determined mainly by large values of μ, while for large, negative values of q the sum is decided by few small values of μ. Therefore, this method allows for different values of q to reflect different values of the measure μ.
Then, if the distribution of the measure μ is scale invariant, the relationship between $\chi_q(\varepsilon)$ and different scales ε follows a power law for any value of q:

$$\chi_q(\varepsilon) \propto \varepsilon^{\tau(q)} \tag{2.9}$$

The exponent $\tau(q)$ can be evaluated as the slope of $\chi_q(\varepsilon)$ versus ε in a log-log plot. I calculated the slope using a least squares regression. It is important to be careful in this step, since the distribution of μ may not be scale invariant for all the scales, at certain values of ε the relationship of $\log(\chi_q(\varepsilon))$ versus $\log(\varepsilon)$ may not be linear. Therefore, $\tau(q)$ can only be evaluated where the distribution of μ is scale free, as long as this is true for a certain range of scales ε [Scheuring and Riedi, 1994]. In this case, I observed that

scale invariance for the lower values of μ is not present for small sizes of ε (figure 3.1), hence, the minimum value used for the regression was a size $\varepsilon = 16$.

Then, it is possible to obtain the Hölder exponent α and the multifractal spectrum $f(\alpha)$ by a Legendre transform [Mandelbrot, 1989]:

$$\alpha(q) = \frac{\partial\tau(q)}{\partial(q)} \qquad \text{and} \qquad f(\alpha(q)) = \alpha(q)q - \tau(q) \tag{2.10}$$

Also, is important to check in which range the moments are defined [Arenas and Chorin, 2006].
The moments of order q for any function are defined as:

$$\langle X^q \rangle = \int x^q f(x) dx$$

High-order moments are not defined when the tails display a power law. If the lower tail follows a power law ($f(\mu) = a\mu^\beta$), its contribution to the q-moment will be:

$$\langle X^q \rangle = \int_0^{\mu_m} \mu^q f(\mu) d\mu = \int_0^{\mu_m} \mu^q a\mu^\beta d\mu =$$

$$a\int_0^{\mu_m} \mu^q \mu^\beta = \frac{a}{q+\beta+1}\left[\mu^{q+\beta+1}\right]_0^{\mu_m} \tag{2.11}$$

where β in this case is the slope of the histogram of all values of μ, in logarithmic scale. This will only take finite values for $q > -\beta - 1$, so in the other case, the moments will be undefined ($\langle X^q \rangle \to \infty$).

2.1.2 The cumulative probabilities method

Also, we tried to approximate the multifractal spectrum directly from the definition given by Mandelbrot [1989], which is the non cumulative distribution of α.
From equation 2.2 we can directly calculate the Hölder exponents:

$$\alpha = \frac{-\log(\mu_{mn})}{\log(L/\varepsilon)} \tag{2.12}$$

Mandelbrot [1989] states that at the limit $\varepsilon \to 0$ the noncumulative probability (which enters the expression for $\Psi(\alpha)$ in the equation 2.5), and the cumulative distribution function of α converge. This limit is meaningful for mathematical fractal objects, but not for empirical or even simulated data. This is the reason why to calculate $f(\alpha)$, Mandelbrot introduces a correction term to the cumulative version of equation 2.4:

$$f(\alpha_i) = \frac{\log(N_{\alpha_i})}{\log(L/\varepsilon)} + \frac{\log(2)}{\log(L/\varepsilon)} \tag{2.13}$$

Where N_{α_i} is the accumulated amount of α_i, which will vary according:

$$N_{\alpha_i} = \begin{cases} \sum_{0}^{\alpha_i} n(\alpha_i) & \text{if} \quad \alpha_i \leq D_E. \\ \\ \sum_{\alpha_i}^{\alpha_{max}} n(\alpha_i) & \text{if} \quad \alpha_i > D_E. \end{cases}$$

Where $n(\alpha_i)$ is the amount of a certain α. That is, the amount of α smaller of than α_i while α is below D_E, in this case $D_E = 2$, and vice versa.

2.2 Temporal evolution of the model

In order to study the temporal evolution of the model, I calculated several variables over time. The time steps are not constant, they correspond tho the intervals between two fire events. Hence, "time" is not linear in this series, among other reasons because lightning strikes have a random component.

The lattice started with all values $r_i^{ij} = 0$. And there were a total of 47 942 fires simulated, therefore the calculations where done on 23 972 occasions.

I calculated:

1. The Shannon entropy, S, (detailed above: equation 2.7)
2. The correlation dimension, C_d, (equation 2.8).
3. Cheng [1994] proposed that the multifractal spectrum, as it is a convex function, can be summarized as $\tau''(1)$, which can be approximated as:

$$\tau''(1) \approx \tau(2) - 2\tau(1) + \tau(0) \tag{2.14}$$

I used this index as a simple measure of the convexity of the multifractal spectrum in the time evolution only. More information about $\tau''(1)$ can be found in Cheng [1999].

4. And also the burnt area since the last fire, BA.

2.3 The empirical data

In order to test the results obtained with the model I used real landscape data. The area studied is the boreal forests of central Alaska, for some reasons:

- The boreal regions are among the few that still preserve a natural, undisturbed state, with a (relatively) little intervention by humans, and therefore it is more likely that the natural dynamics of the ecosystems are more intact than in other ecorregions [Foley et al., 2005].
- The boreal forests are also subject to a fire regime that seems to have an endogenous component [Niklasson and Granström, 2000]. The area selected for the study had an important amount of fires, which can be appreciated in figure 2.1.
- The study developed by Pueyo [2007] was done in boreal forests, in the Canadian province of Alberta.
- The best data publicly available (to my knowledge) is developed by the United States Geological Survey (USGS) for their territory.

As r_i is a theoretical concept, I needed to use a similar variable which could be found in the available data.
Many forest fire models used to accurately predict the behaviour of a certain fire, such as the popular model FARSITE, are based on the mathematical model developed by Rothermel [1972], which summarizes different aspects of the landscape as a spread rate r_s. This r_s is a measure of how fast the fire spreads to a neighbour area, and can be interpreted as the vulnerability of the neighbouring area to catch fire, either from an existing fire or from the first spark that lights up the fire.
We could also expect that if lightning strikes on areas with low r_s, there are few chances that it ignites a fire. And an existing fire is less likely to spread further in this area.

Therefore this rate of spread r_s can be interpreted as a proxy for the probability of fire propagation of the SOCFUS model, r. As we will see in section 2.3.1, where the model Rothermel [1972] is detailed, this r_s has also some external components (wind, moisture) and internal (fuel type, slope) which are also common features with the SOCFUS model, making it feasible a better comparison of this theoretical model with the reality.

2.3.1 From fuel types to rates of spread

The equations of the mathematical model of Rothermel [1972] (RFM) are complex, with many parameters to be calculated, but here I will explain only the main equation:

$$r_s = \frac{I_R \xi (1 + \phi_w + \phi_s)}{\rho_b \epsilon Q_{ig}} \tag{2.15}$$

Where I_R is the *reaction intensity*, that is, the energy release rate of the fire front. It can be approximated as the rate of change of organic matter from solid to gas (as it is burned). Therefore it depends on the amount of burnable materials, the heat content of those materials, and a very important component: the moisture content of the fuel.

- ξ is the *propagating flux ratio*. It basically depends on the compactness of the fuel bed, and on a parameter that quantifies the fuel particle size.
- ϕ_w and ϕ_s are the *wind and slope coefficients*, respectively.
- ρ_b is the *fuel bulk density*.
- ϵ is the *effective heating number*, which relates the size of the fuel particles with the amount of heat required to ignite.
- And Q_{ig} is the *heat of preignition*, that is, the amount of energy required to burn a certain material. It depends basically on the fuel moisture.

The notation I used is taken from RFM, as well as the definition of the parameters. More details on the equations and how to apply them to real data can be found on his work.

It is important to highlight some aspects of this equation. It has some components which are intrinsic of the landscape and the fuel type, and others that depend on environmental conditions:

- I_R and Q_{ig} depend heavily on moisture content, either in a direct or indirect way. And ϕ_w depends only on wind speed. Therefore those parameters can be related to r_e of the SOCFUS model.

- ξ, ρ_b and ϵ are dependent on different components of the fuel type, either the compactness of the material, the particle size, the heat content... Those parameters are then related to the r_i component of the SOCFUS model.

Then, in order to obtain a parameter similar to r_i from empirical data, I calculated the r_s, but keeping this parameter's dependence on the environment constant. To do so, I used the *Standard fire behaviour fuel models* developed by Scott and Burgan [2005]. They classify the possible fuels found in the ecosystems in 40 categories, and give the parameters for each fuel required to use the RFM model (equation 2.15).

So, with available empirical data that used the same classification as Scott and Burgan [2005], and using equation 2.15, I obtained a parameter, r_s, comparable to the probability of fire occurence, r, of the SOCFUS model.
Furthermore, I used the same environmental scenario and weather conditions for all fuel types in order to see only the effect of the internal component of the fuels, hence to approximate a r_i (at least relative to the other fuels). To do this, I used the moisture values according to the *low* scenario (D2L2) described in Scott and Burgan [2005], a wind speed of 5 m/s and no slope. All the results given in this work will be based in those conditions.

2.3.2 Acquisition and processing of the data

The data used were obtained from the *Landscape Fire and Resource Management Planing Tools* (LANDFIRE) (www.landfire.gov), developed by the USGS and other agencies from the United States for their territory. There is a wide range of geospatial products freely available related to terrestrial ecology and forest fires, among them, the 40 fire behaviour models of Scott and Burgan [2005].

The area of study, as mentioned in section 2.3, is in central Alaska (figure 2.1). It is a rectangular area delimited by the following coordinates:
The upper left corner (155.20 W, 63.55 N), and bottom right corner (64.53 N, 149.17 W). It has a size of 298.95 km x 117.84 km, which comprises an area of 35 228.3 km^2.

In the north, it is delimited by the Yukon and Tanana rivers, and in the south by the Alaskan mountain range.

The area is almost completely covered by boreal forest, with few wetlands near the river systems. On the southern limit, where the Alaskan mountain range begins, there are areas with some alpine vegetation.

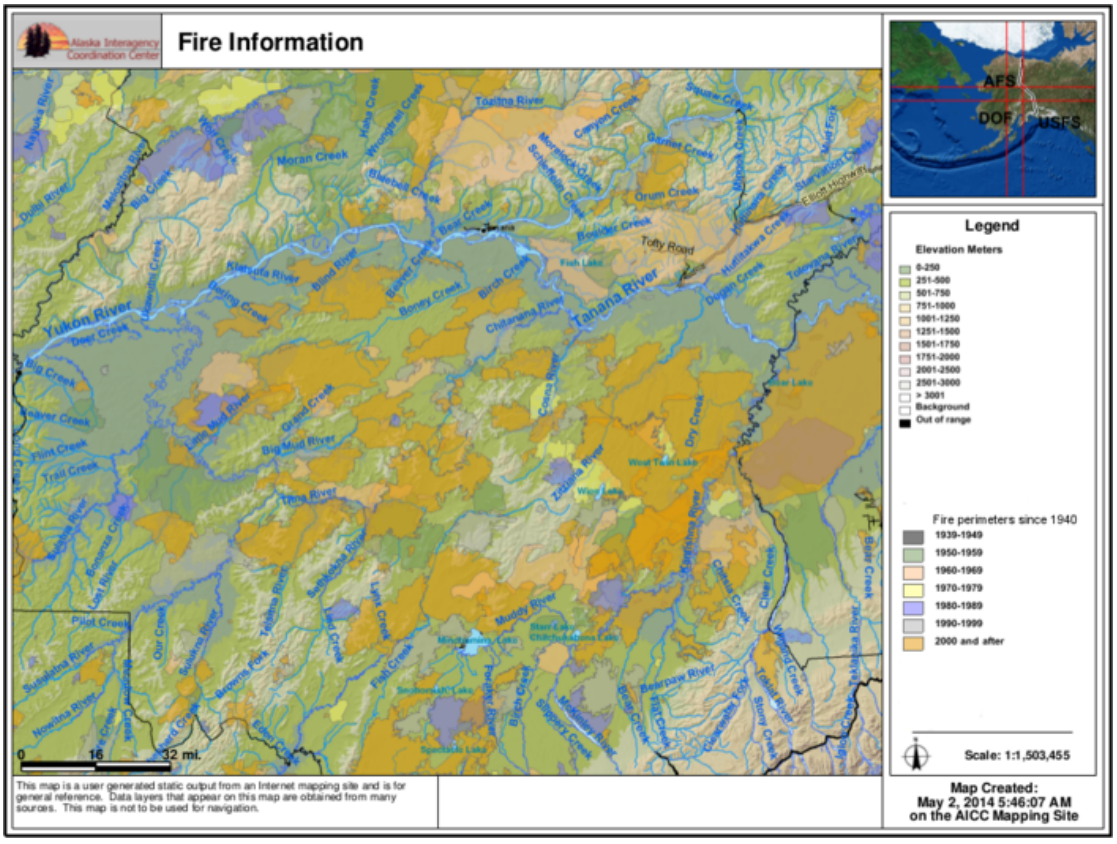

FIGURE 2.1: Map of the study area of Alaska (red rectangle). Also as polygons, the historical fires recorded in that area. Map created by the *Alaska Interagency Coordination Center*, and modified by the author.

The data was downloaded as a shape file, with a resolution of 30 m. Each pixel has a value corresponding to a certain type of fuel. The shape file was exported to an ASCII file using the software ArcGIS Desktop, obtaining a matrix of 9965x3928, with $39.14 \cdot 10^6$ values. The relationship between the fuel code and the fuel type is found in Scott and Burgan [2005]: a number between 100 and 204, and if it is non burnable a pixel value of 9999. With this information, and the r_s values obtained for each fuel type, a new matrix is obtained where the values represent the rate of spread r_s, with constant environmental conditions as described in section 2.3.1.

This matrix then is used to calculate the multifractal spectrum of real ecosystems, using

the central part where the forest is more continuous, without the presence of the rivers in the north and the mountain range in the south. As in the model, the size of the square matrix to calculate the multifractal spectrum is 2048x2048, so I could study four different zones of the landscape.

2.4 The critical value of the SOCFUS model

As it is clear in equation 2.2, if the landscape is multifractal, each value of μ, i. e. a certain amount of fuel, has a particular singularity exponent, α. And the frequency of each α, if looked at different sizes ε, follows a power law, with an exponent $f(\alpha)$, which defines the multifractal spectrum (eq. 2.3).
We can stablish then a relationship of a certain value of μ with a *fractal dimension* $f(\alpha)$.

Besides, Pueyo [2007] showed in his work that there is also a relationship between the environmental conditions, r_e, and the distribution of the fire size, summarized as the power law exponent, β. To compare it with the multifractal spectrum, the parameter required is r_i, which can be obtained from:

$$r_i = r_c - r_e \tag{2.16}$$

Where r_c is the critical value of r.

r_c is the critical point where percolating fires happen. That is an infinite fire that would never cease if the lattice was infinitely large. To understand it better, imagine a fire that starts at one side of the lattice, and has to reach the other side. For this to happen, it is necessary that all the lattice is covered by a certain amount of cells with a large probability to spread the fire. The critical value will be the mean value of all cells of the lattice. In a simple percolating model it corresponds to $r_c = 0.5$. Pueyo [2007] estimated $r_c \approx 0.53$ for the SOCFUS model, very close to the theoretical value. To check if this threshold is useful to identify fire-prone clusters, I will calculate the histogram of all r values of all cells burnt during a simulation with SOCFUS model.
It should reveal the value of r that was burnt more often, possibly r_c.

Chapter 3

Results

3.1 Multifractal structure of the forest

Here I present the results that show the multifractal structure of the forest. The first part will deal with the theoretical landscape originated by the SOCFUS model and then I will present the results for the empirical data.

3.1.1 Multifractal structure of the landscape emerged from the SOCFUS model

Following the method of moments, described in section 2.1.1, I obtained the relationship between the mass-partition function of μ, $\chi_q(\varepsilon)$, and the size of the box, ε, for $-10 \leq q \leq +10$. This range of q is sufficient, as it will be clear in figure 3.2. The resolution for the values of q is 0.01, so I did this calculation for 2000 different values of q. However, in figure 3.1 I represent only 20 values for a better visualization.

In figure 3.1 it is possible to see that for large, negative values of q the slope is not linear when ε is small. That means that small μ values do not show scale invariance when we look the lattice with high resolution. Therefore, for negative values of q I estimated the slope only for $\varepsilon \geq 16$.

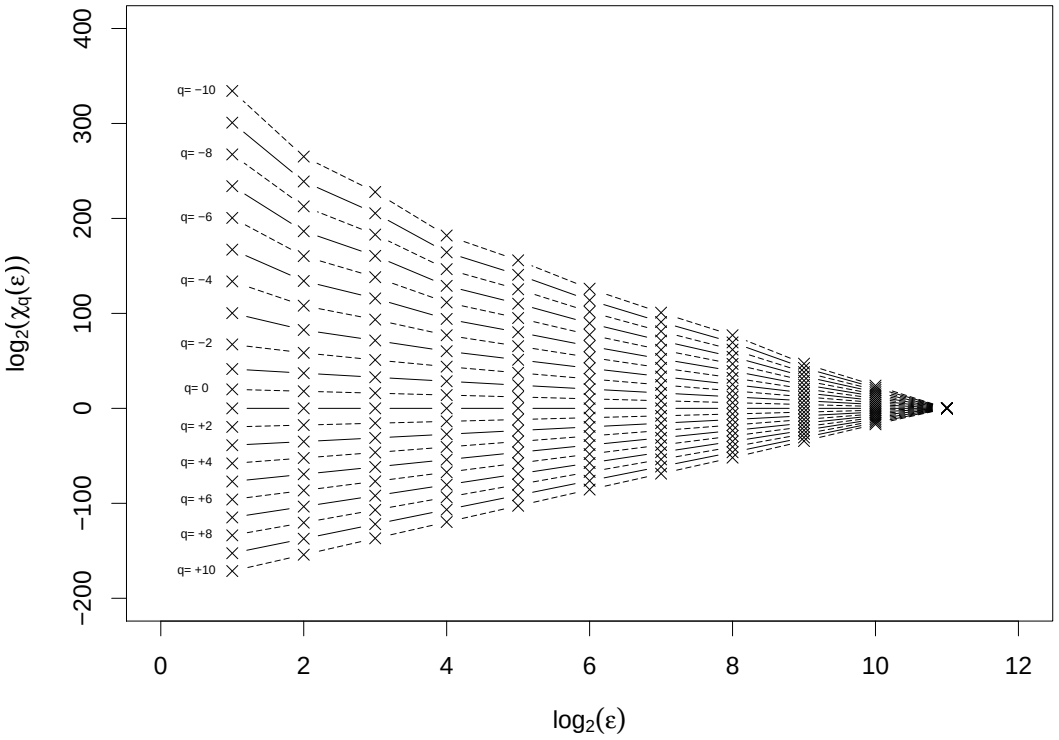

FIGURE 3.1: Log-log plot of $\chi_q(\varepsilon)$ vs ε, for $-10 \leq q \leq +10$. Note that for large, negative values of q the slope is not linear.

The slope of $\chi_q(\varepsilon)$ versus ε is $\tau(q)$, for each value of q (equation 2.9). The regression coefficients, R, obtained by least-squares regression were:

for $-10 \leq q < 0$ R ≤ -0.99963

for $0 \leq q \leq 10$ R $\geq +0.99998$

With the values of $\tau(q)$, I obtained the Hölder exponent, α, and $f(\alpha)$ using the Legendre transform (equation 2.10).

The details of the operations are explained in section 2.1.1.

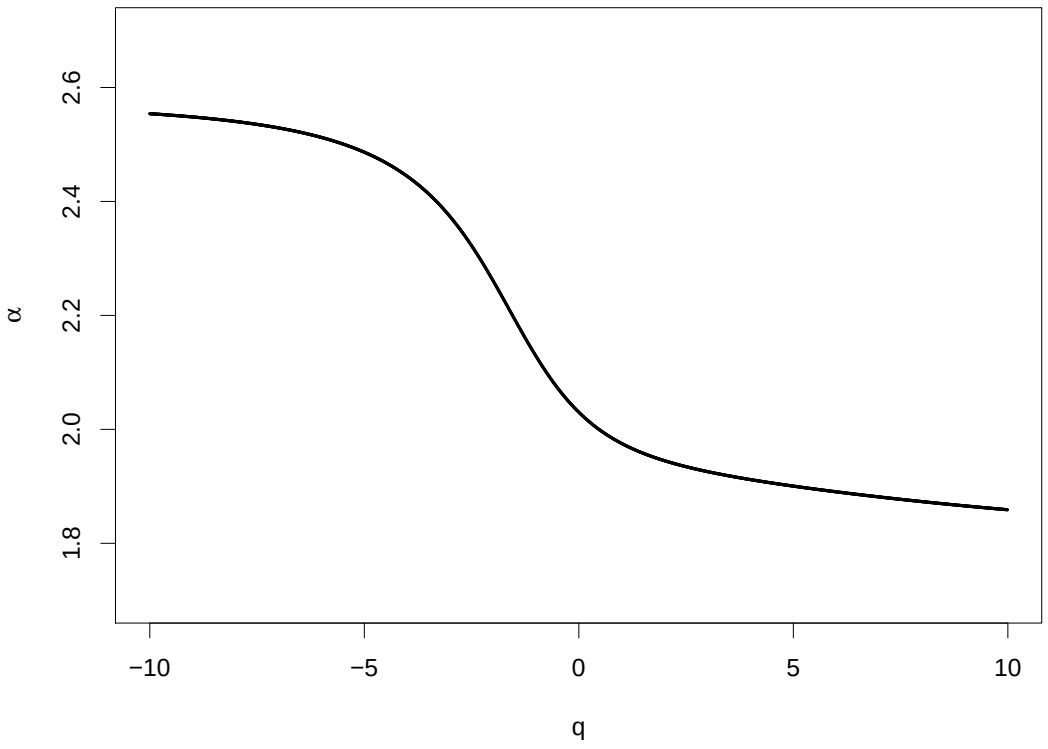

FIGURE 3.2: Plot of the Hölder exponents, α versus q.

In figure 3.2, I show the different values of α depending on q, which are related to different values of μ. Therefore, small values of q, which are caused by small values of μ, have large values of α.
And the opposite: cells with a high value of μ (detected with a high q) are related to small α.

Also, it is clear that for large absolute values of q (either positive or negative) the values of α do not vary substantially. That is, most of the α are defined for the central values of q. Therefore studying the range of $-10 \leq q \leq +10$ is more than enough to study this lattice.

This is important as some studies suggest that high order moments may not be defined [Arenas and Chorin, 2006], it will not be our case for positive values of μ, as they are truncated at $\mu = 0.7/T_{r_i}$, and all moments on that area will be defined. However, there could be problems at the lower tail of the data, with negative values of q.

To check if high-order moments are not defined, I considered the following: if the lower tail follows a power law, and according to equation 2.11, the moments of order q will be finite if $q > -\beta - 1$, and in the other case, the moments will be undefined ($\langle X^q \rangle \to \infty$).

I estimated β from the histogram shown in figure 3.3, $\beta = 4.055$. So this first survey of our data suggests that problems may arise for moments of order $q < -5$, which corresponds just to the higher values of α. Therefore, affecting just a minor part of the spectrum, and in no case the values of μ related with the fire risk (high values of (μ)).

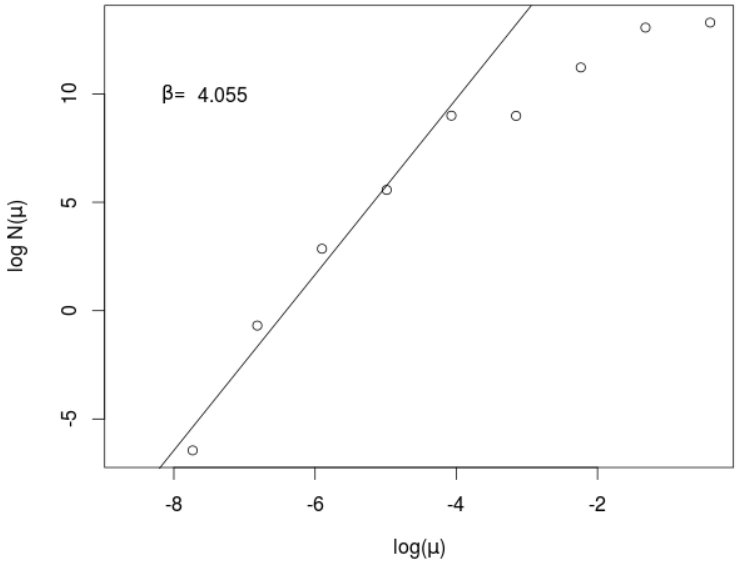

FIGURE 3.3: Histogram of μ for the matrix of the simulated landscape, in logarithmic scale. The slope of the histogram, β, is positive.

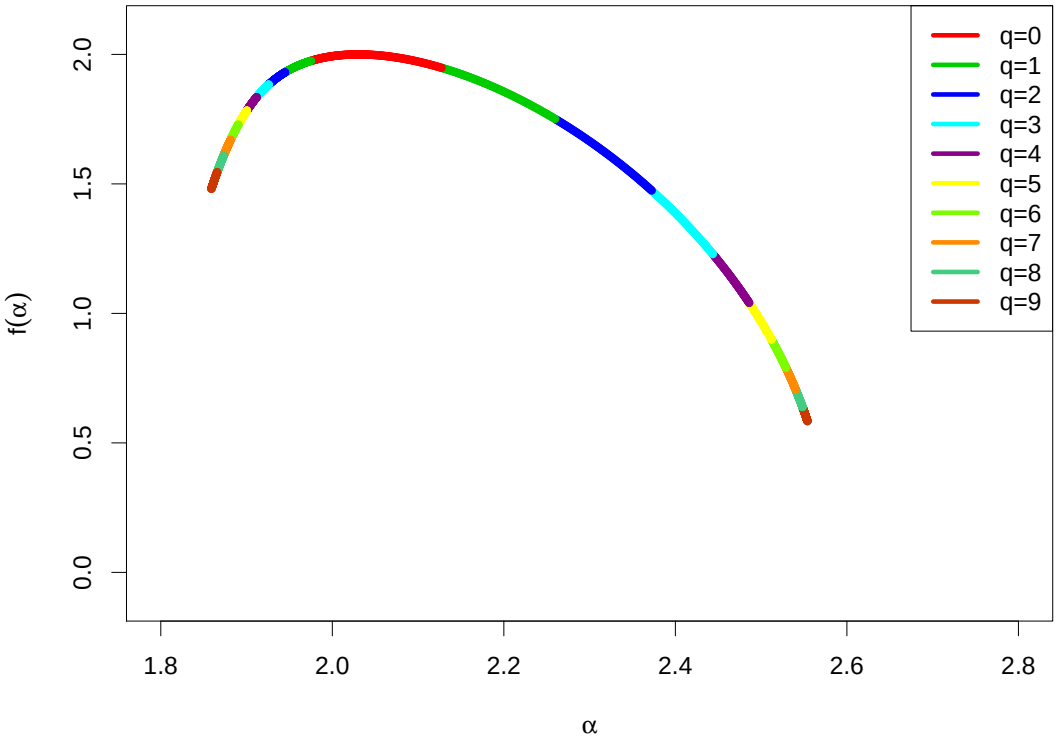

FIGURE 3.4: The multifractal spectrum, α vs $f(\alpha)$. The colours represent different values of q, the same colour either for positive or negative q. Note that $q = 10$ is not shown as these values correspond to the same as $q = 9$.

And finally, as stated above, using the Legendre transform I obtained the multifractal spectrum, α vs $f(\alpha)$. As expected, it has a convex shape, and the maximum value of $f(\alpha)$ is 2, the Euclidean dimension of the system, which also coincides with the singularity value of 2.

Also, the spectrum is clearly unbalanced to the right (larger values of α). This is probably caused by a constraint of the model. As explained in section 1.2.2, the values that r_i can take are constrained to $r_i \in [0, r_\infty]$, where $r_\infty = 0.7$. This causes that, as the forest grows, the amount of fuel arrives to this threshold that cannot be trespassed, and therefore many cells have this value.

Seen in terms of the multifractal formalism, lower values of α, which are caused by larger values of μ, have a larger fractal dimension ($\approx f(\alpha)$). That is, this measure is more common in space. This is for $\alpha > 2$, in the other side of the function smaller values of α have lower $f(\alpha)$.

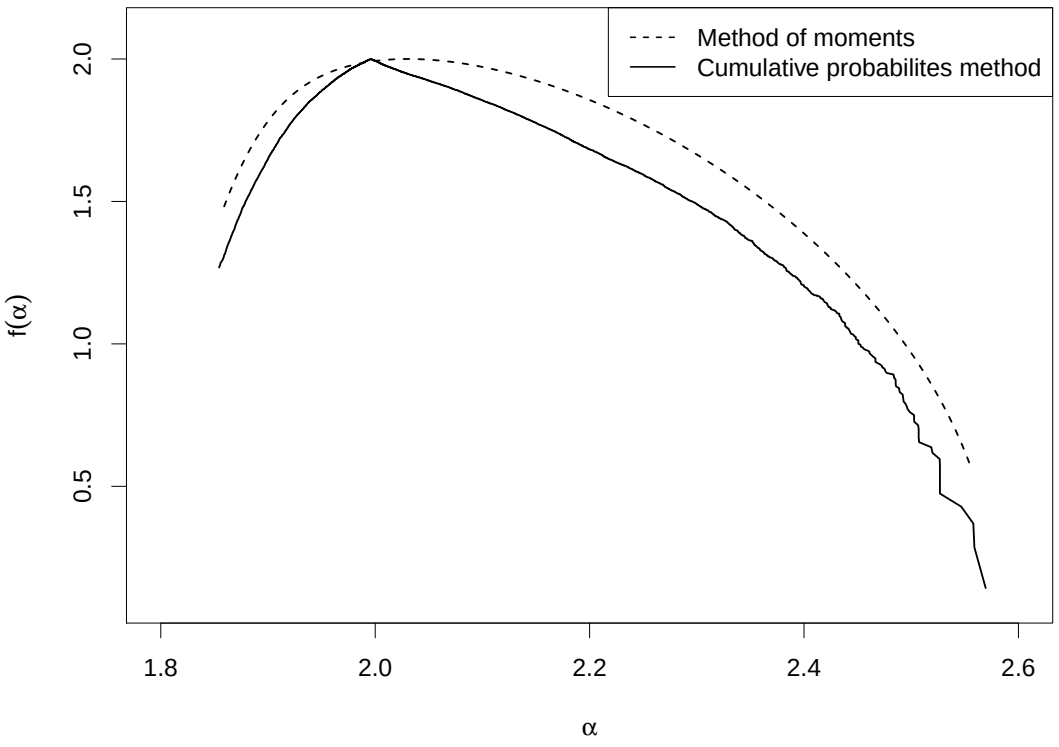

FIGURE 3.5: Comparison of both methods to calculate the multifractal spectrum, the method of moments and the cumulative probabilities method.

In figure 3.5 I show the multifractal spectrum calculated using the most common approach, the method of moments, and also using the method the cumulative distribution function of α [Mandelbrot, 1989]. The calculations were done according the equation 2.13.

3.1.2 Multifractal structure of fuel types in boreal forests in Alaska

The same analysis was performed on the study zone of Alaska, but in this case four areas were studied (figure 3.6, numbered from 1 to 4). Note that the zone is not homogeneous, as there are different geographical features (hills, mountains in the south, rivers and lakes in the east) that condition the type and distribution of fuels.

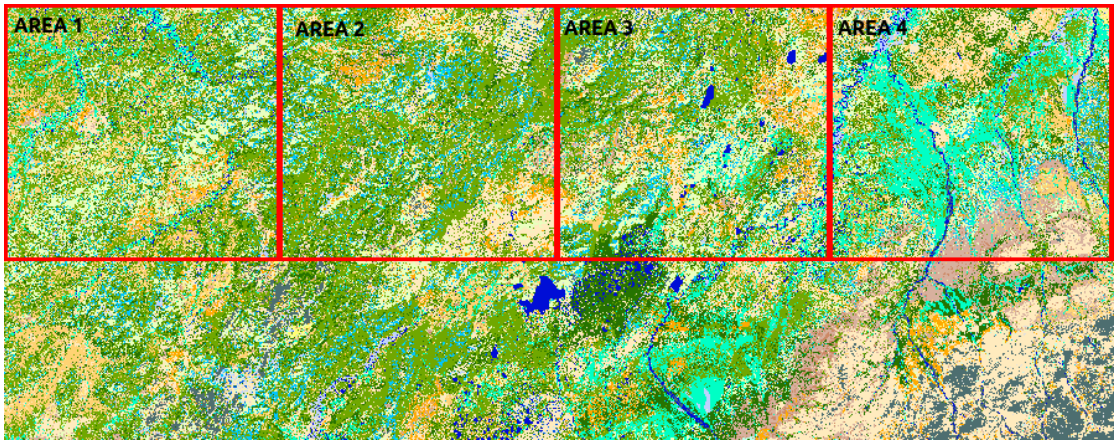

FIGURE 3.6: Map of fuel types of the zone studied in Alaska, the four zones are marked in red.

The diversity of the landscape has implications in the following results, as some parts will show different multifractal patterns. Area 1, 2 and 3 are quite similar, while area 4 has a large amount of a specific type of fuel, related to river and wetlands. When I calculated the power law that relates the partition function $\chi_q(\varepsilon)$ and the scale we are using, ε, in the area 4 I found scale invariance only for a large size of the box (figure 3.7 **b**).

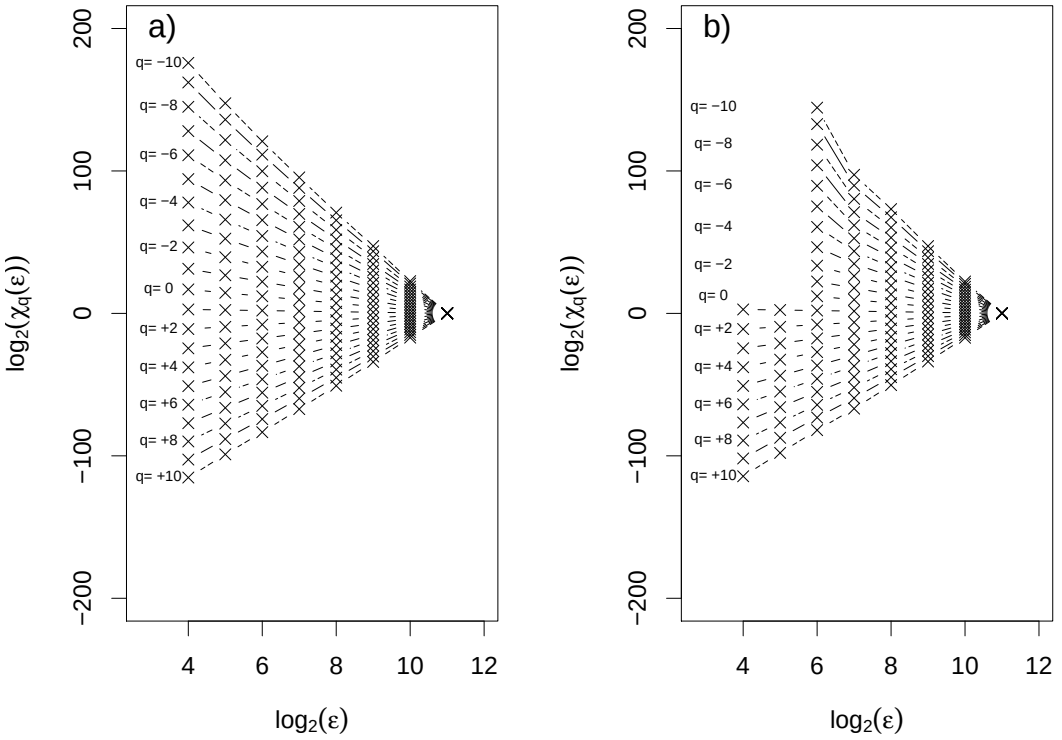

FIGURE 3.7: Log-log plots of $\chi_q(\varepsilon)$ vs ε from the empirical data. **a** Corresponds to area 1 of the zone studied, while **b** corresponds to zone 4. Note that **b** do not show a scale invariance as clear as **a**.

In figure 3.7 I show the power laws for a portion of values of q. **a** is from area 1, while **b** is from area 4.

The minimum correlation coefficient found, R, for each zone are:

Area 1 $|R| \geq 0.9999$

Area 2 $|R| \geq 0.9998$

Area 3 $|R| \geq 0.9993$

Area 4 $|R| \geq 0.9908$

The area 4, as it has a correlation coefficient much lower than the others, will not be used for further comparison.

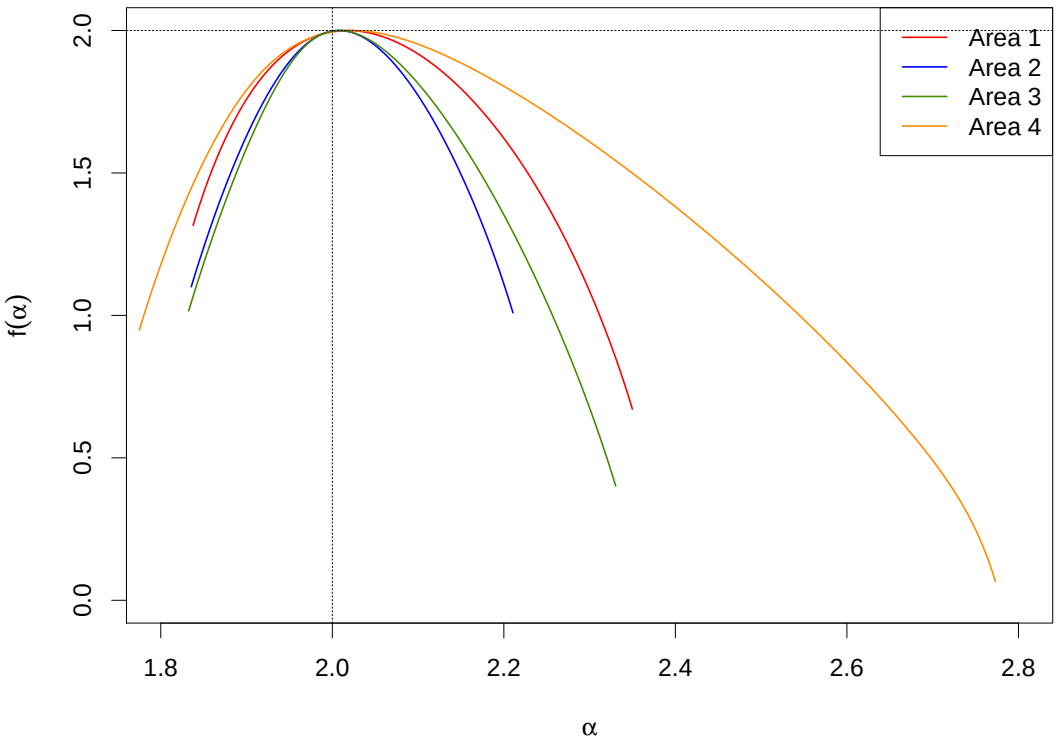

FIGURE 3.8: The multifractal spectrum, α vs $f(\alpha)$, obtained from different zones of the landscape in Alaska.

Clearly, the landscape from the boreal forest in Alaska is also multifractal. Furthermore, it has as well a small unbalance to larger values of α, in a similar way as the multifractal spectrum of the SOCFUS model, although not so strong.

It is important to highlight that, due to the poor quality of the power law of the area 4, the spectrum of this area is very different than the others. As stated above, I will discard this area as it has some geographical features that make it less representative of the boreal forest region.

3.2 Temporal evolution of the SOCFUS model

In figure 3.9, I show the temporal evolution of the model, summarized as 4 different variables, the convexity of the multifractal spectrum $\tau''(1)$, where a smaller number represents a narrow multifractal spectrum, and close to 0 a very broad one. The Shannon

entropy, S, which if it is lower corresponds to a more diverse landscape; the correlation dimension, C_d, where a higher value indicates a larger correlation between two points of the lattice; and finally, the surface burned from the previous fire, BA. For the details of the calculations see section 2.2.

If we consider either, S, $\tau''(1)$ or C_d as indicators of self organisation, is clear that until a certain amount of fires has taken place the system is not diverse enough to maintain a certain complexity. In this case, the amount of fires required is ≈ 2200 (figure 3.11). After that, the system shows multifractal patterns.
However, the shape of the multifractal spectrum, $\tau''(1)$, varies over time in a wide range (figure 3.9), showing some clear oscillations at the beginning, but never reaching a steady state. The mean value was $\tau''(1) = -0.0216$.

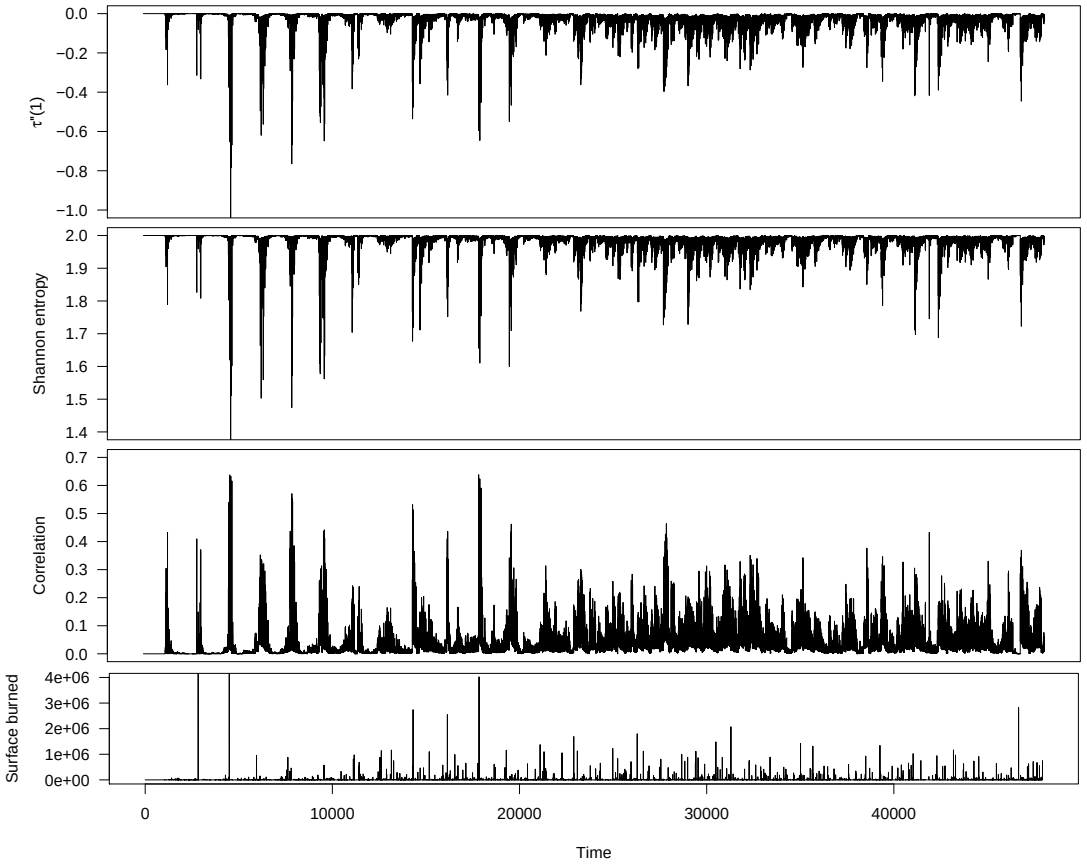

FIGURE 3.9: Temporal evolution of the SOCFUS model, as the multifractality index $\tau''(1)$, the Shannon entropy, S, the correlation dimension, C_d and the surface burned from the previous fire, BA_f (In this latter plot, the first two large fires are truncated; the surface burned was about $9{\cdot}10^6$, twice the size of the axis).

The same patterns are visible in the other variables, S and C_d. This is clear if we calculate the Pearson correlation, $R_{x,y}$, between those time series:

$$R_{\tau''(1),C_d} = -0.9317$$
$$R_{\tau''(1),S} = 0.9899$$
$$R_{C_d,S} = -0.8741$$

Hence, all of those variables are clearly correlated to each other. To show it in more detail, figure 3.10 shows the relationship between $\tau''(1)$ and S.

It is clear that the entropy decreases when the system has a multifractal spectrum more convex. But the system tends to go to states with higher entropy, which corresponds to larger heterogeneity of the landscape, precisely where is more resistant to large fires. It is important to note that $\tau''(1)$ measures the convexity of the multifractal spectrum, so when it is very convex, the range of α present in the system is shorter than if $\tau''(1)$ is close to 0. So the system tends to go to a state with more variety of α.

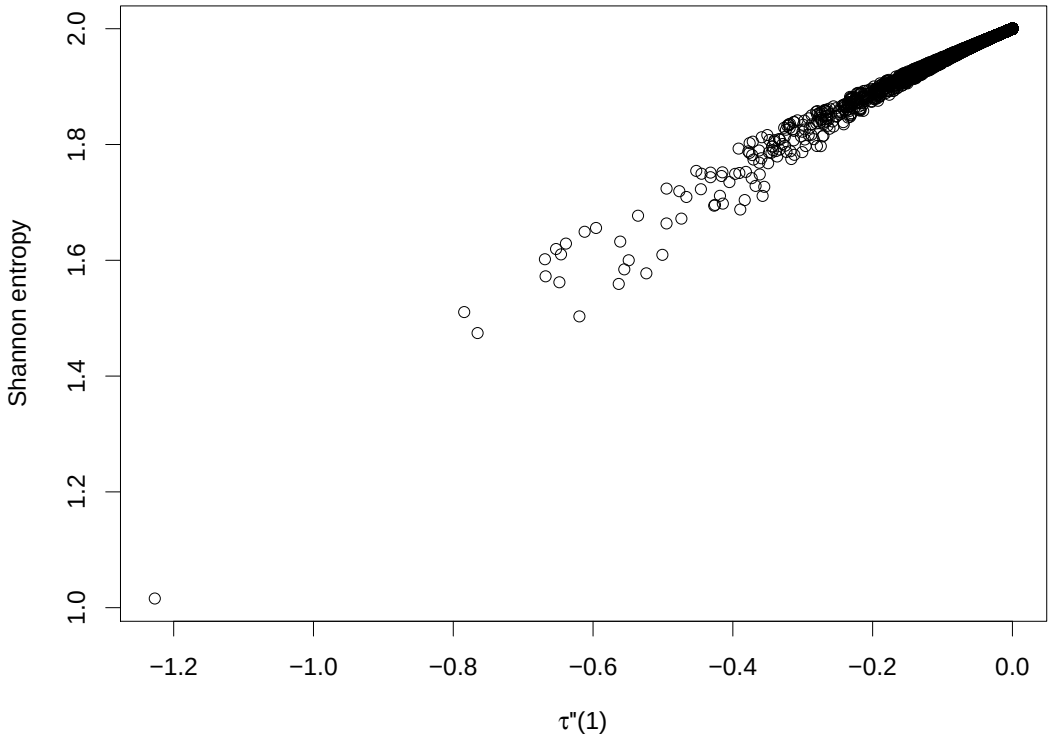

FIGURE 3.10: Relationship between $\tau''(1)$ and S.

In order to trace the origin of the self-organisation of the system, I calculated the multifractal spectrum at different moments, close to the critical instant where the first important fire occurs (≈ 2200).

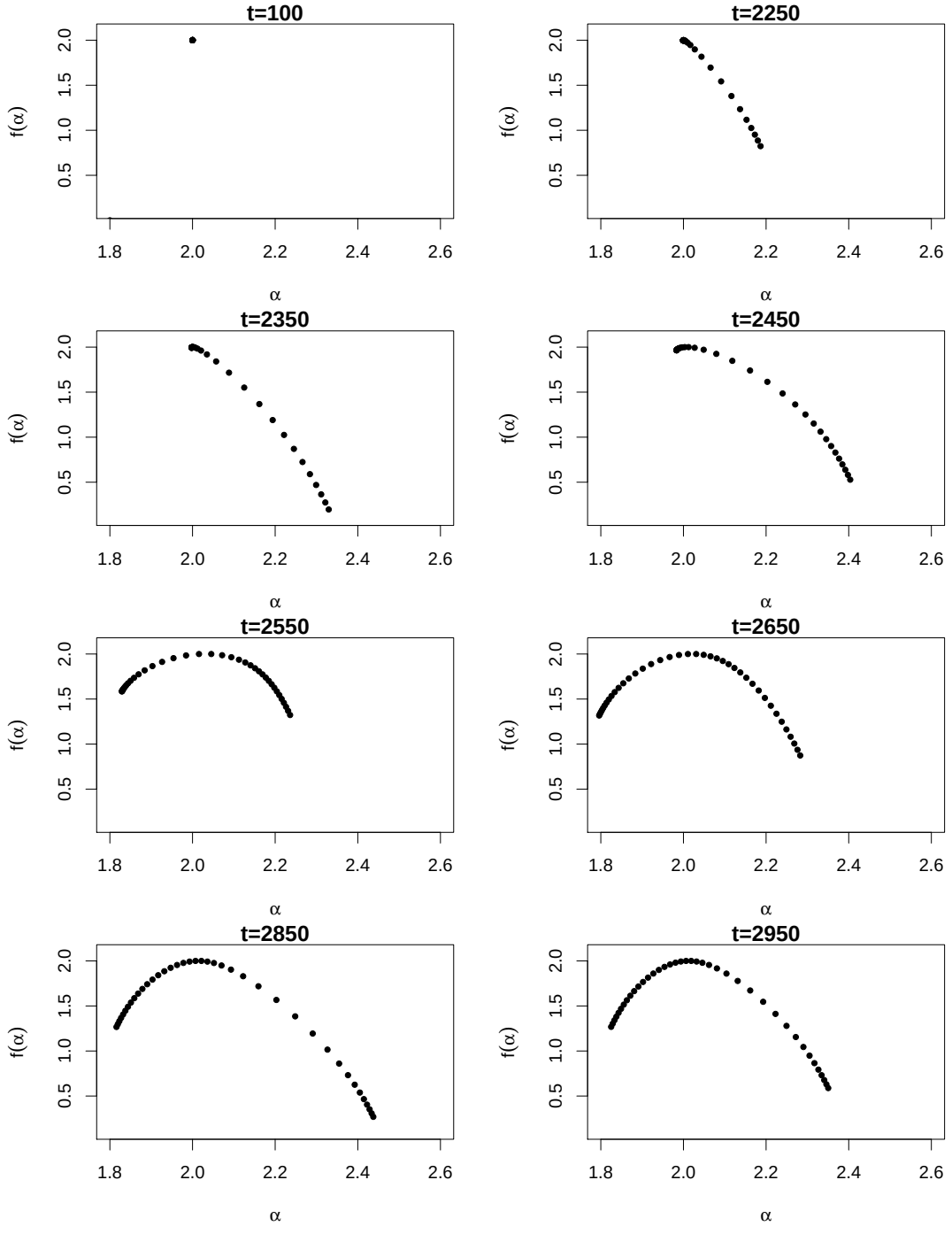

FIGURE 3.11: The emergence of multifractality: the multifractal spectrum calculated at different time steps.

3.3 From the multifractal spectrum to the power law exponents

3.3.1 The critical value of the SOCFUS model

The critical value of the SOCFUS model corresponds to $r_c \approx 0.5$, for the whole system. Specific patches should also burn more easily when their local r cross the critical threshold. In order to see if this is the case I calculated the histogram of all r values of all cells burnt during a simulation with SOCFUS model (figure 3.12).
There should be visible the value of r that was burnt more often, probably, the critical value of the SOCFUS model.

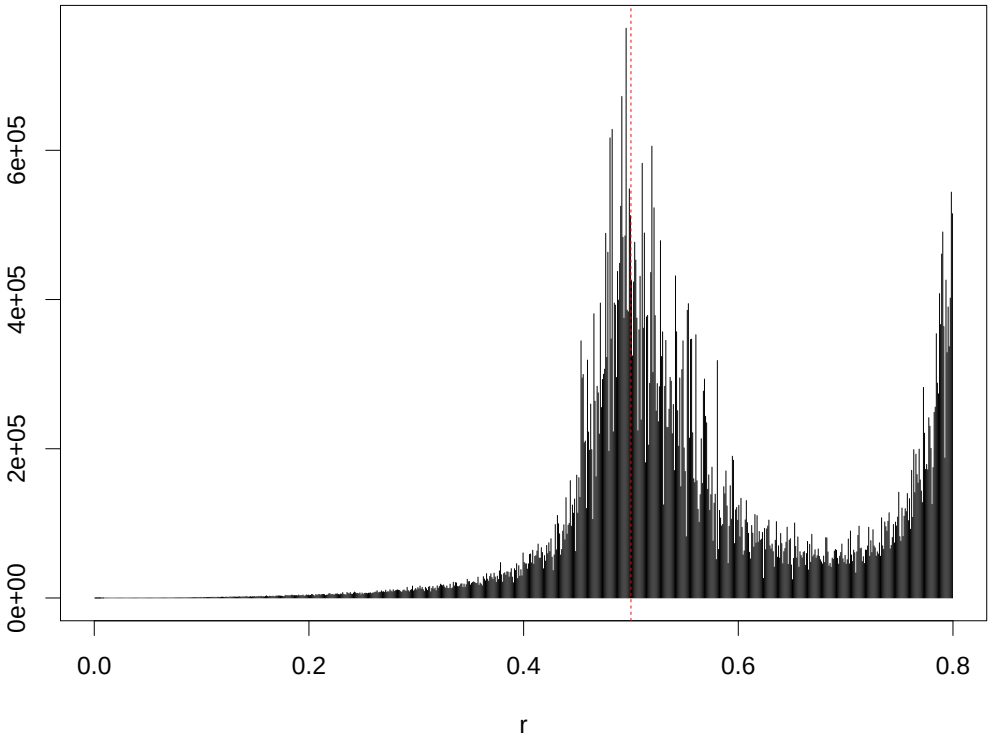

FIGURE 3.12: Histogram of r, for all cells that burnt during a simulation of the SOCFUS model. The red, dotted line marks the value $r = 0.5$.

In figure 3.12, it is clear that the most frequent value is ≈ 0.5. There is as well an anomalous accumulation at 0.8, but this is due to the restriction of the model that the

maximum value of r_i is 0.7, so this is over-represented than in the natural dynamic. Hence, the critical value of the model is also the value burnt more often, $r_c = 0.5$.

3.3.2 Exponents of the power laws and the decomposition of the multifractal spectrum

Pueyo [2007] found an interesting relationship between the exponent of the power law, β, and r_e (figure 1.2).

Furthermore, I found that this relationship can be explained by a second order polynomial function ($R^2 = 0.9989$), the equation is shown in figure 3.13.

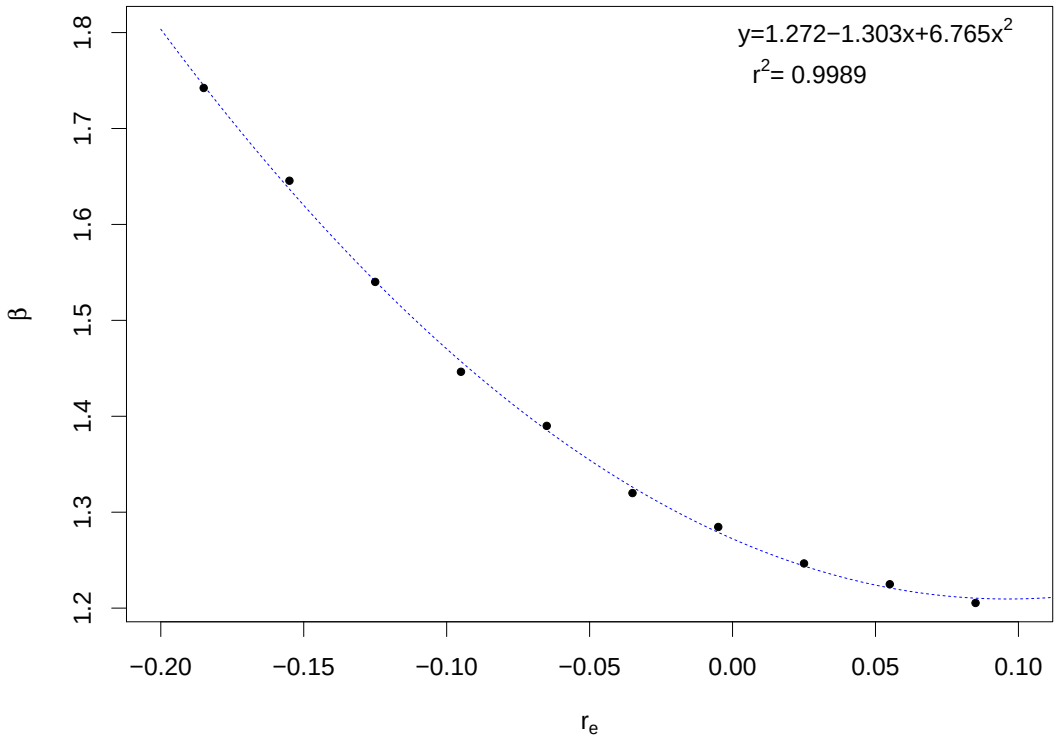

FIGURE 3.13: Relationship between r_e and β.

With this data, we can use equation 2.16 with $r_c = 0.5$, to find r_i for a certain β.

And now, using equation 2.1, we get a value of μ, which can be expressed as a Hölder exponent α, with equation 2.12.

TABLE 3.1: Equivalence between different parameters.

β	r_e	r_i	μ	α
1.742	-0.185	0.685	$5.94{\cdot}10^{-7}$	1.880
1.646	-0.155	0.655	$5.68{\cdot}10^{-7}$	1.886
1.540	-0.125	0.625	$5.42{\cdot}10^{-7}$	1.892
1.446	-0.095	0.595	$5.16{\cdot}10^{-7}$	1.899
1.390	-0.065	0.565	$4.90{\cdot}10^{-7}$	1.906
1.319	-0.035	0.535	$4.64{\cdot}10^{-7}$	1.913
1.285	-0.005	0.505	$4.38{\cdot}10^{-7}$	1.920
1.247	0.025	0.475	$4.12{\cdot}10^{-7}$	1.928
1.225	0.055	0.445	$3.86{\cdot}10^{-7}$	1.937
1.205	0.085	0.415	$3.60{\cdot}10^{-7}$	1.946

The next step, to obtain $f(\alpha)$ from α, is straightforward with the multifractal spectrum from figure 3.4.

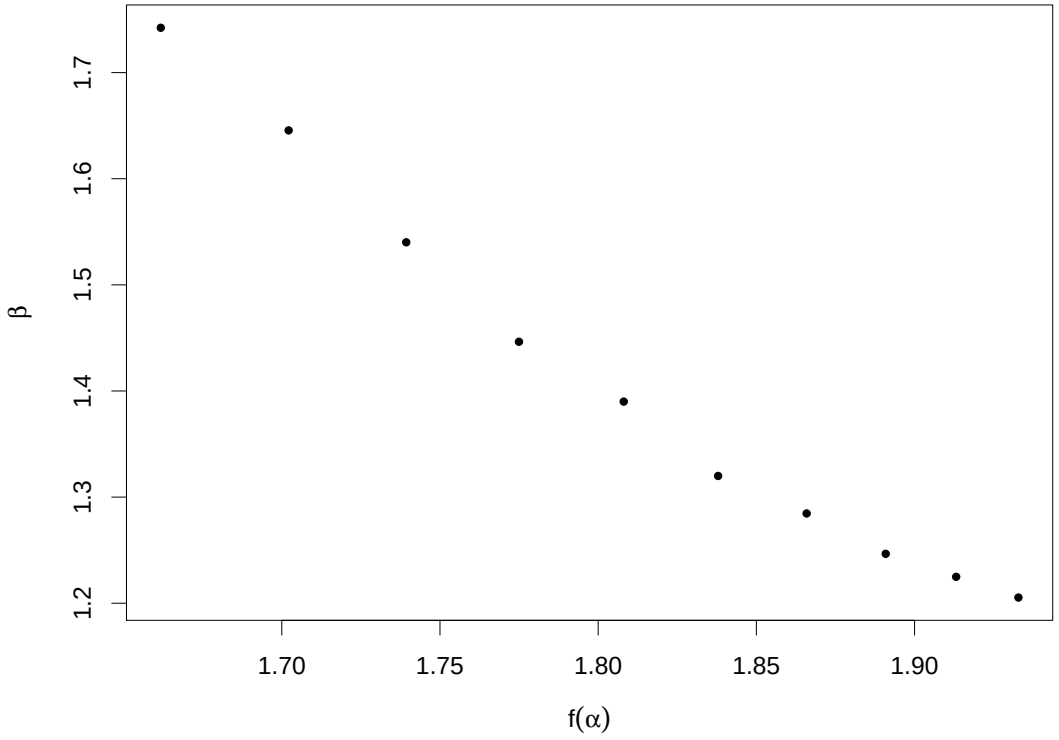

FIGURE 3.14: Relationship between β and $f(\alpha)$.

Another interesting relationship I found is between the environmental conditions, r_e, and the multifractal spectrum, $f(\alpha)$.

The implications of all those results are important, and will be discussed on the next chapter.

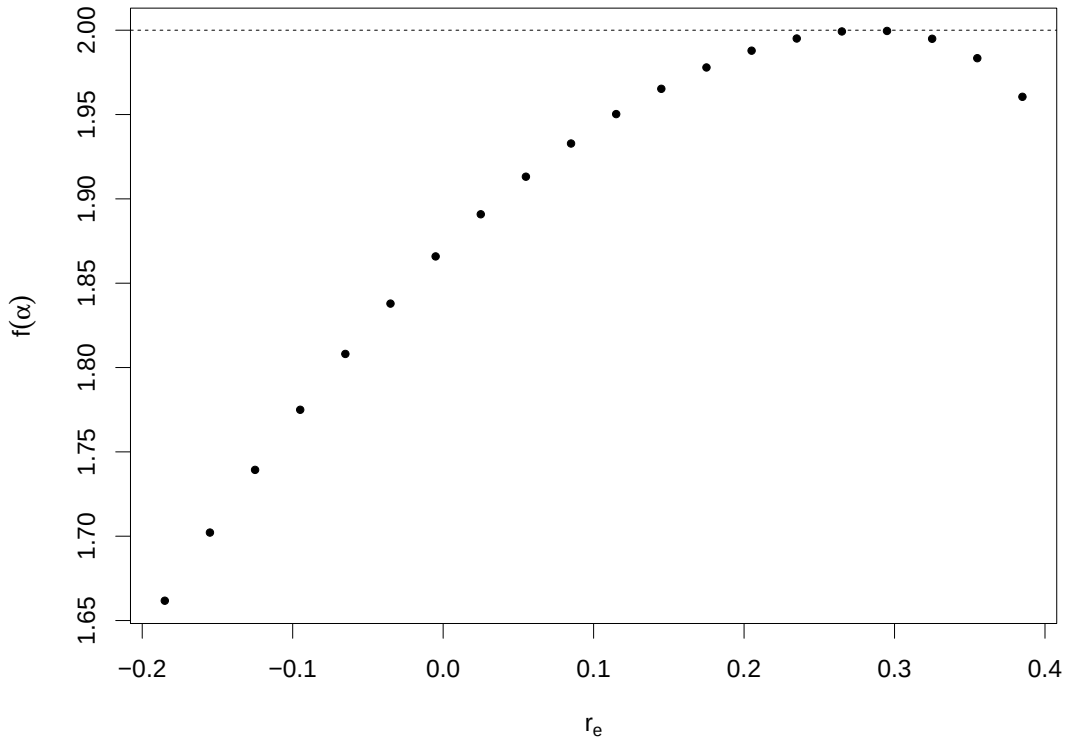

FIGURE 3.15: Relationship between r_e and $f(\alpha)$. The value of $f(\alpha) = 2$, that corresponds to the Euclidean dimension, is marked with a dotted line.

Chapter 4

Discussion

4.1 Multifractal patterns in ecosystems

4.1.1 Multifractality of the landscape of self-organised ecosystems

In the previous chapter, I showed that some terrestrial ecosystems such as forests, under a fire regime which is intrinsic to many biomes, are self-organised, showing clear multifractal patterns. This was shown for a a simple model that reproduces fire dynamics in a lattice, but more interestingly, empirical data from a large area of central Alaska display similar patterns.

Multifractal structures in the landscape of terrestrial ecosystems were already observed: in forest gaps in rain forests [Solé and Manrubia, 1995], in canopy height in a longleaf pine savanna [Drake and Weishampel, 2001], land use in China [Wang et al., 2010], diversity of plant species in subtropical forests [Wei et al., 2013], but this study is the first to show a clear relationship with fire. An interesting study related with SOC and forest fire was done by Sinha-Ray et al. [2001], with another variant of the FF model, although the multifractal analysis performed was only for the distance between trees, something completely unrelated with the fire. Therefore our point of view is quite different and approaches the mechanism of the model directly. However, it is suggestive that the shape of the multifractal spectrum obtained by Sinha-Ray et al. [2001] is similar to this study, supporting that universal properties are present in the model.

Also, in figure 3.5 I compare the method that is more widely used to calculate the multifractal spectrum, the method of moments, and the approach of multifractals as a cumulative distribution function of α [Mandelbrot, 1989]. We should not forget that, as many mathematical definitions, the computation of the multifractal spectrum through the method of moments is just an approximation, which sometimes dilutes the meaning of the measure. This is the reason I calculated it using the cumulative probabilities method, as it is the approach that comes closer to the concept of multifractality. Mandelbrot [1989] already stated that this method has strong limitations to calculate the multifractal spectrum, but it is useful to support the method of moments and specially, the interpretation of the multifractal spectrum as a the probability distribution of α.

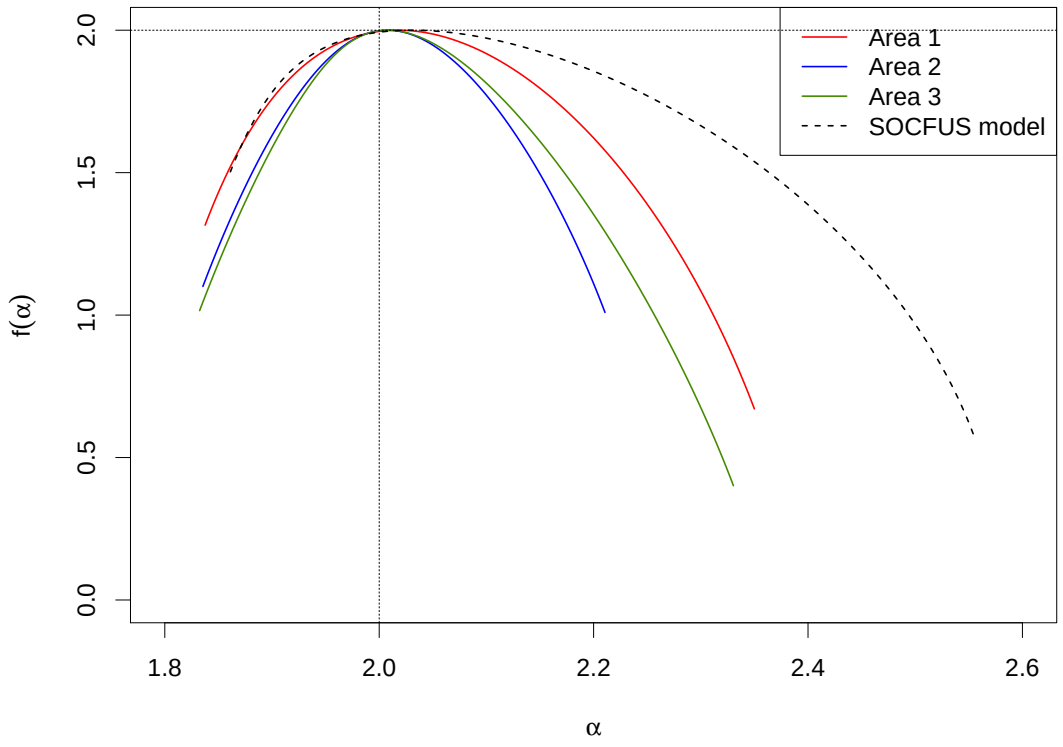

FIGURE 4.1: The multifractal spectrum, α vs $f(\alpha)$, obtained from different zones of the landscape in Alaska.

In figure 4.1, I compare the multifractal spectrum from three areas of Alaska and the spectrum obtained from the landscape originated in the SOCFUS model. There are some differences in the results from empirical data, specially for larger values of α, but is important to note that as shown in section 3.1.1, large values of α, which are related

to low values of μ show a poorer scale invariance, so some variability is normal, specially from empirical data. Of course, our hypotheses were qualitative and a quantitative correspondence was not our expectation. So it is important to highlight that the shapes are very similar.
It is very interesting, though, that for small values of α all the spectrums show a similar pattern; this is important as this part of the spectrum is related with high values of μ, and is the area more vulnerable to fire.

To really understand the multifractal spectrum, we may think about $f(\alpha)$ as the fractal dimension of a given α, which is related to a certain amount of fuel.
A large $f(\alpha)$ means a higher fractal dimension of that α, that means that the μ related to that α covers relatively well the space. In our example, the landscape from the SOCFUS model and the Area 1 from Alaska are very similar: their fuels with larger μ are distributed in similar patterns. On the other hand, Area 2 and 3 from Alaska have lower values, i. e. the distribution of areas with high fuel is less common.
This approach can be interesting to apply when studying the landscape, specially for fire management.

4.1.2 Multifractality of a SOC system over time

In figure 3.11 I show the instants immediately after the multifractal spectrum is detected (t=2250).
Until then, all fractal dimensions are collapsed to a single value, 2. After the critical instant, the part of the function with $\alpha > 2$ starts to develop and present scale invariance; this is the area related with small values of μ.
And then, around t=2450, the other side of the function with $\alpha < 2$, starts to unfold and become self similar at different scales, and importantly, with varying intensities for different values of μ (multifractality). This delay happens because the system needs extra time to have a certain amount of cells with large values μ, in order to have cells with small α.
After that, the multifractal spectrum shows some oscillations to both sides. In fact, the spectrum shows differences at any different times where it is calculated. This is clear if we look at the measure $\tau''(1)$ in the figure 3.9. Therefore, as the system is dynamic, so is the multifractal spectrum that defines it.

One interesting study about the evolution of a multifractal system over time was done by Saravia et al. [2012a,b]. They studied the ecological succession in periphyton communities, and although the systems and mechanisms that drives them are very different, there is a common feature regarding multifractality: There is a sudden increase of multifractality at the beginning (a wider multifractal spectrum), and then variations at a lower level, which I also observed (figure 3.9), [Saravia et al., 2012a].

4.2 Environmental conditions decompose the multifractal spectrum

Pueyo [2007] found that different environmental conditions, either on a model that simulates forest fires or real boreal forests, are related to different power laws of the fire size distribution. This relationship is shown in fig 1.2, where r_e is the environmental conditions in the model and FWI is proxy to that parameter in empirical data. The power law is characterized by the exponent β.

This has important implications, as it supports that boreal forests are self-organised due to forest fires. But more importantly, shows that SOC systems are susceptible to external forcings, being expressed as different power laws. Also, from a practical point of view, he related a fact that was already known (warmer, drier conditions make large fires more probable), with a mathematical expression that explains it, and allows to know the probability of fire sizes under a certain weather.

His analyses were developed in one dimension, the time series of forest fires sizes. This thesis is one step forward of Pueyo [2007], gathering the three dimensions that compose the model and the reality. As the starting point is that forests are self-organised, showing scale invariance, the obvious direction to approach this issue is to use fractal and multifractal tools. As shown in the previous section, the forest is arranged in a multifractal structure, where different probabilities of fire are present, and each of them distributed in a unique pattern, a fractal dimension $f(\alpha)$. Those probabilities can be expressed as Hölder exponents (equation 2.2), therefore a certain probability of fire r, is related to a $f(\alpha)$.

So merging both ideas, we see that different power laws are related to different $f(\alpha)$. This means that given some environmental conditions, which causes a certain fire size

distribution with the parameter β, act on certain $f(\alpha)$ (figure 3.14). So each fractal dimension is susceptible to different external conditions.
To sum up, the environment decomposes the multifractal spectrum of the forest.

The natural world is formed by a large variety of fractal shapes and structures, and until now the fractal geometry and multifractal formalism have proven very useful to describe it. Here I show that they are not only passive descriptors, but they play an important role in ecosystems, being the transmission chain between external forcings and the internal, self-organising processes of the systems.

4.2.1 Implications for climate change: the megafire

There is also an interesting relationship between different values of environmental conditions, r_e, with the fractal dimension, $f(\alpha)$ (figure 3.15). It is clear that as r_e decreases, the set of α affected by fire corresponds to a lower $f(\alpha)$, and this means that these values are less present in the lattice than other with higher $f(\alpha)$.
But the important aspect of this relationship is that there is a certain value of r_e that affects the zones corresponding to a $f(\alpha) = 2$, which is the maximum value that the multifractal spectrum can take, and corresponds to the Euclidean dimension of the landscape. The consequences of this is that when $r_e \approx 2.7$, the layer susceptible to the fire is the whole lattice ($f(\alpha) = 2$), and a percolating fire is feasible with those conditions. In the context of climate change as the weather becomes more severe (in the model means that r_e increases gradually) this megafire becomes more likely.

This supposition is only according to the model, but there are three facts that make it feasible in the reality:

1. The relationship between the environmental conditions and β is similar in empirical data and the model [Pueyo, 2007].

2. The multifractal patterns found in the real forests are comparable to the landscape emerged from the model (figure 4.1).

3. There are evidences that boreal forests in Alaska are now crossing a major threshold [Mann et al., 2012], where vast areas of forests that before were not affected

by fire, are now becoming vulnerable. They also observed a decrease of β over the last 20 years, with more large fires.

Then, with those evidences, I hypothesize that in the coming years there will be certain environmental conditions that will trigger a megafire in boreal forests, such as the ones found in Alaska. Those large fires will cause an abrupt shift in the ecosystem, and after that it will self-organise into a new state.
This hypothesis is plausible, as phase shifts are already observed in many ecosystems, going rapidly from a certain state of the system to another [Scheffer et al., 2001] due to a loss of resilience. Here I suggest that the resilience, in some systems, is related to the multifractal patterns that compose the system, and when the environmental forcing changes fast enough and reaches the maximum $f(\alpha)$ a phase shift happens. This change should be fast enough, as if it is gradual the system may be able to shift to a more stable state.

4.2.2 Insights for forest management

The characterisation of the landscape using the multifractal formalism is also useful for forest management, specially related with forest fire. I cannot go deep enough as it is beyond the scope of this thesis, but there are some ideas that may be useful for this research field.

Studying the landscape through multifractal tools allows us to capture the inherent complexities of ecosystems, revealing some essential components, and embracing all scales: from a single tree to a regional scale. In principle would be possible, given certain environmental conditions, to know which type of fuel and which areas are more susceptible to the fire.
Also, knowing the distribution and sizes of patches with a given type of fuel, would be possible to intervene on the structure of the landscape to manage fire regimes.

It is also feasible to represent the landscape as the Hölder exponents, α, instead of the fuel map, and if we consider the fire as a turbulent diffusive process, some multifractal tools can reveal hidden details beneath the forest. For example, a recent study on the multifractal signature of sea surface temperature was used to reconstruct the global sea currents, a turbulent process, with a very high resolution [Turiel et al., 2009]. I suggest

that a similar approach can be applied to forest fires, but instead of currents, predicting the evolution of a fire on a given landscape of singularities.

Chapter 5

Conclusions

In this thesis, I show that one system that is self-organised, in this case a landscape under a forest fire regime, is arranged in multifractal patterns. This is shown not only for a simple model that simulates forest fires [Pueyo, 2007], but also for empirical data of boreal forests in Alaska. This is important to understand self-organisation processes and specially the ones that happen in the natural world.

I also studied the temporal evolution of the system, showing an important correlation between different variables that represent it. Some self-organized systems show fractal structures not only spatially but also temporally [Solé et al., 2001]. I did not do the calculations, but the power law of fire sizes found by Pueyo [2007] suggests that the system may be multifractal in the three dimensions studied.

Moreover, I show that the environmental conditions that are present in the SOCFUS model, which cause different power laws of fire sizes, are closely related to the multifractal structure of the forest. This implies that multifractal patterns on ecosystems are not just a way to describe them, but an important component in the relationship of the ecosystems with the environment.
I also hypothesize that, as the multifractal spectrum makes the system sensitive to the environmental conditions, if the perturbation is large enough to reach $f(\alpha) = 2$, which corresponds to the Euclidean dimension, an infinite, percolating fire is feasible, causing an abrupt shift in the system. This must be taken into account in a context of climate change, as there are already signs in Alaska that the ecosystem is stressed, near the threshold [Mann et al., 2012].

The multifractal formalism is poorly understood when used by ecologists or biologists, but may have large implications to understand the world and provide information of several key features, such as the arrangement of features in the space, their interaction with the environment, and the storage of information. The work developed on turbulent flows from a multifractal point of view [Turiel et al., 2009], must be taken into account to many diffusive processes in ecology.

Bibliography

FP Agterberg. Multifractal modeling of the sizes and grades of giant and supergiant deposits. *International Geology Review*, 6(2):2012, 1995. doi: 10.1127/gtm/6/1996/131.

Alexandre Arenas and Alexandre J Chorin. On the existence and scaling of structure functions in turbulence according to the data. *Proceedings of the National Academy of Sciences of the United States of America*, 103(12):4352–4355, 2006.

Markus Josef Aschwanden. *Self-Organized Criticality Systems*, volume 1. Open Academic Press, Berlin, Warsaw, 2013, 483pp., Warsaw, volume 1 edition, 2013.

Per Bak and Kim Sneppen. Punctuated equilibrium and criticality in a simple model of evolution. *Physical review letters*, 71(24):4083–4086, 1993.

Per Bak, Chao Tang, and Kurt Wiesenfeld. Self-organized criticality. *Physical review A*, 1988.

Qiuming Cheng. *Multifractal modelling and spatial analysis with GIS: Gold potential estimation in the Mitchell-Sulphurets Area, northwestern British Columbia*. PhD thesis, 1994.

Qiuming Cheng. Multifractality and spatial statistics. *Computers & Geosciences*, 25 (9):949–961, November 1999. ISSN 00983004. doi: 10.1016/S0098-3004(99)00060-6. URL http://linkinghub.elsevier.com/retrieve/pii/S0098300499000606.

André Dauphiné. *Fractal Geography*. Wiley, 2013. ISBN 9781848213289.

J.B. Drake and J.F. Weishampel. Simulating vertical and horizontal multifractal patterns of a longleaf pine savanna. *Ecological Modelling*, 145(2-3):129–142, November 2001. ISSN 03043800. doi: 10.1016/S0304-3800(01)00398-2. URL http://linkinghub.elsevier.com/retrieve/pii/S0304380001003982.

B. Drossel and F. Schwabl. Self-organized criticality in a forest-fire model. *Physica A: Statistical Mechanics and its Applications*, 191(1):47–50, September 1992. ISSN 0031-9007. doi: 10.1103/PhysRevLett.69.1629. URL http://link.aps.org/doi/10.1103/PhysRevLett.69.1629.

Jonathan A Foley, Ruth DeFries, Gregory P Asner, Carol Barford, Gordon Bonan, Stephen R Carpenter, F Stuart Chapin, Michael T Coe, Gretchen C Daily, Holly K Gibbs, and Others. Global consequences of land use. *Science*, 309(5734):570–574, 2005.

U Frisch and G Parisi. Turbulence and predictability in geophysical fluid dynamics and climate dynamics. *Proceedings of the International School of Physics "Enrico Fermi", Course LXXXVIII*, 1985.

Thomas C. Halsey, Mogens H. Jensen, Leo P. Kadanoff, Itamar Procaccia, and Boris I. Shraiman. Fractal measures and their singularities: The characterization of strange sets. *Physical review. A*, 34(2):1601, August 1986. ISSN 1050-2947.

Christopher L Henley. Statics of a "self-organized" percolation model. *Physical review letters*, 71(17):2741, 1993.

Gerardo Iovane, E Laserra, and F S Tortoriello. Stochastic self-similar and fractal universe. *Chaos, Solitons & Fractals*, 20(3):415–426, 2004.

Plamen CH Ivanov, Luís A Nunes Amaral, Ary L Goldberger, Shlomo Havlin, Michael G Rosenblum, Zbigniew R Struzik, and H Eugene Stanley. Multifractality in human heartbeat dynamics. *Nature*, 399(6735):461–465, 1999.

Andrey Nikolaevich Kolmogorov. Dissipation of energy in locally isotropic turbulence. In *Dokl. Akad. Nauk SSSR*, volume 32, pages 16–18, 1941.

Benoit B Mandelbrot. How long is the coast of Britain. *Science*, 156(3775):636–638, 1967.

Benoit B Mandelbrot. *The Fractal Geometry of Nature*. 1982.

Benoit B Mandelbrot. Multifractal measures, especially for the geophysicist. *Fractals in geophysics*, 1989. URL http://link.springer.com/chapter/10.1007/978-3-0348-6389-6_2.

DH Daniel H Mann, TS Scott Rupp, Mark A Olson, and Paul A Duffy. Is Alaska's Boreal Forest Now Crossing a Major Ecological Threshold? *Arctic, Antarctic, and Alpine Research*, 44(3):319–331, 2012. URL http://instaar.metapress.com/index/R8G406172P32386R.pdf.

Ramon Margalef. Our biosphere. *Ecology Institute*, 1997.

K. Nagel and E. Raschke. Self-organizing criticality in cloud formation? *Physica A: Statistical Mechanics and its Applications*, 182(4):519–531, April 1992. ISSN 03784371. doi: 10.1016/0378-4371(92)90018-L.

Mats Niklasson and Anders Granström. Numbers and sizes of fires: long-term spatially explicit fire history in a Swedish boreal landscape. *Ecology*, 81(6):1484–1499, June 2000. ISSN 0012-9658. doi: 10.1890/0012-9658(2000)081[1484:NASOFL]2.0.CO;2.

Zeev Olami, Hans Feder, and Kim Christensen. Self-organized criticality in a continuous, nonconservative cellular automaton modeling earthquakes. *Physical Review Letters*, 68(8):1244–1247, February 1992. ISSN 0031-9007. doi: 10.1103/PhysRevLett.68.1244. URL http://link.aps.org/doi/10.1103/PhysRevLett.68.1244.

Salvador Pueyo. Self-Organised Criticality and the Response of Wildland Fires to Climate Change. *Climatic Change*, 82(1-2):131–161, February 2007. ISSN 0165-0009. doi: 10.1007/s10584-006-9134-2. URL http://link.springer.com/10.1007/s10584-006-9134-2.

Salvador Pueyo, Paulo Maurício Lima de Alencastro Graça, Reinaldo Imbrozio Barbosa, Ricard Cots, Eva Cardona, and Philip M Fearnside. Testing for criticality in ecosystem dynamics: the case of Amazonian rainforest and savanna fire. *Ecology letters*, 13(7):793–802, July 2010. ISSN 1461-0248. doi: 10.1111/j.1461-0248.2010.01497.x.

Richard C Rothermel. A mathematical model for predicting fire spread in wildland fuels. *Forest, Intermountain*, 1972.

Leonardo Ariel Saravia, Adonis Giorgi, and Fernando Momo. Multifractal growth in periphyton communities. *Oikos*, 121(11):1810–1820, November 2012a. ISSN 00301299. doi: 10.1111/j.1600-0706.2011.20423.x. URL http://doi.wiley.com/10.1111/j.1600-0706.2011.20423.x.

Leonardo Ariel Saravia, Adonis Giorgi, and Fernando Momo. Multifractal spatial patterns and diversity in an ecological succession. *PLoS one*, 7(3):e34096, January 2012b. ISSN 1932-6203. doi: 10.1371/journal.pone.0034096.

Marten Scheffer, Steve Carpenter, Jonathan A Foley, Carl Folke, and Brian Walker. Catastrophic shifts in ecosystems. *Nature*, 413(6856):591–596, 2001.

István Scheuring and Rudolf H. Riedi. Application of multifractals to the analysis of vegetation pattern. *Journal of Vegetation Science*, 5(4):489–496, August 1994. ISSN 11009233. doi: 10.2307/3235975. URL http://doi.wiley.com/10.2307/3235975.

Joe H Scott and Robert E Burgan. Standard fire behavior fuel models: a comprehensive set for use with Rothermel's surface fire spread model. *The Bark Beetles, Fuels, and Fire Bibliography*, page 66, 2005.

Proshun Sinha-Ray, Luís Borda de Água, and Henrik Jeldtoft Jensen. Threshold dynamics, multifractality and universal fluctuations in the SOC forest-fire: facets of an auto-ignition model. *Physica D: Nonlinear Phenomena*, 157(3):186–196, September 2001. ISSN 01672789. doi: 10.1016/S0167-2789(01)00300-1. URL http://linkinghub.elsevier.com/retrieve/pii/S0167278901003001.

Ricard V Solé and Susanna C Manrubia. Are Rainforests Self-organized in a Critical State? *Journal of theoretical Biology*, pages 31–40, 1995.

Ricard V Solé, David Alonso, Jordi Bascompte, and Susanna C Manrubia. On the fractal nature of ecological and macroevolutionary dynamics. *Fractals*, pages 1–24, 2001.

David G. Tarboton, Rafael L. Bras, and Ignacio Rodriguez-Iturbe. The fractal nature of river networks. *Water Resources Research*, 24(8):1317–1322, August 1988. ISSN 00431397. doi: 10.1029/WR024i008p01317. URL http://doi.wiley.com/10.1029/WR024i008p01317.

Antonio Turiel, Conrad J. Pérez-Vicente, and Jacopo Grazzini. Numerical methods for the estimation of multifractal singularity spectra on sampled data: A comparative study. *Journal of Computational Physics*, 216(1):362–390, July 2006. ISSN 00219991. doi: 10.1016/j.jcp.2005.12.004. URL http://linkinghub.elsevier.com/retrieve/pii/S0021999105005565.

Antonio Turiel, Verònica Nieves, Emilio García-Ladona, J. Font, M.-H. M-H Rio, G. Larnicol, E. Garcia-Ladona, J. Font, M.-H. M-H Rio, and G. Larnicol. The multifractal structure of satellite sea surface temperature maps can be used to obtain global maps of streamlines. *Ocean Science Discussions*, 6(1):129–151, January 2009. ISSN 1812-0822. doi: 10.5194/osd-6-129-2009. URL http://www.ocean-sci-discuss.net/6/129/2009/.

De Wang, Bojie Fu, Kangshou Lu, Luxiang Xiao, Yuxin Zhang, and Xiaoming Feng. Multifractal analysis of land use pattern in space and time: A case study in the Loess Plateau of China. *Ecological Complexity*, 7(4):487–493, December 2010. ISSN 1476945X. doi: 10.1016/j.ecocom.2009.12.004. URL http://linkinghub.elsevier.com/retrieve/pii/S1476945X09001330.

Shi-Guang Wei, Lin Li, Zhong-Liang Huang, Wan-Hui Ye, Gui-Quan Gong, Xiao-Yong Zhou, and Ju-Yu Lian. Multifractal analysis of diversity scaling laws in a subtropical forest. *Ecological Complexity*, 13:1–7, March 2013. ISSN 1476945X. doi: 10.1016/j.ecocom.2011.10.004. URL http://linkinghub.elsevier.com/retrieve/pii/S1476945X11000729.